




A mitochondrial FUNDC1/HSC70 interaction organizes the proteostatic stress response at the risk of cell morbidity

Yanjun Li¹, Yanhong Xue², Xiaojun Xu³, Guopeng Wang⁴, Yiqun Liu⁴, Hao Wu¹, Wenhui Li¹, Yueying Wang¹, Ziheng Chen¹, Weilin Zhang¹, Yushan Zhu⁵ , Wei Ji², Tao Xu^{2,3} , Lei Liu^{1,*} & Quan Chen^{1,5,6,**} 

Abstract

Both protein quality and mitochondrial quality are vital for the cellular activity, and impaired proteostasis and mitochondrial dysfunction are common etiologies of aging and age-related disorders. Here, we report that the mitochondrial outer membrane protein FUNDC1 interacts with the chaperone HSC70 to promote the mitochondrial translocation of unfolded cytosolic proteins for degradation by LONP1 or for formation of non-aggresomal mitochondrion-associated protein aggregates (MAPAs) upon proteasome inhibition in cultured human cells. Integrative approaches including csCLEM, Apex, and biochemical analysis reveal that MAPAs contain ubiquitinated cytosolic proteins, autophagy receptor p62, and mitochondrial proteins. MAPAs are segregated from mitochondria in a FIS1-dependent manner and can subsequently be degraded via autophagy. Although the FUNDC1/HSC70 pathway promotes the degradation of unfolded cytosolic proteins, excessive accumulation of unfolded proteins on the mitochondria prior to MAPA formation impairs mitochondrial integrity and activates AMPK, leading to cellular senescence. We suggest that human mitochondria organize cellular proteostatic response at the risk of their own malfunction and cell lethality.

Keywords cellular senescence; mitochondria; mitochondrial quality control; mitophagy; proteostatic stress

Subject Categories Autophagy & Cell Death; Post-translational Modifications, Proteolysis & Proteomics; Protein Biosynthesis & Quality Control
 DOI 10.15252/emboj.201798786 | Received 7 December 2017 | Revised 25 August 2018 | Accepted 4 October 2018 | Published online 27 December 2018

The EMBO Journal (2019) 38: e98786

Introduction

Both protein quality and mitochondrial quality are vital for cellular activity and health. Protein quality is maintained through a coordinated network involving chaperones and two proteolytic systems, the ubiquitin–proteasome and autophagy–lysosome systems (Mizushima *et al*, 2008; Hartl *et al*, 2011; Koga *et al*, 2011). Proteasomes and autophagy share substrates, effectors, and regulators and compensate for one another in times of need (Kaushik & Cuervo, 2015). Chaperones, including heat-shock protein 70 (HSP70) family proteins, which assist the folding/unfolding, assembly/disassembly, and membrane translocation of their clients, as well as sorting them for degradation through the proteasomal or autophagic pathways (Kaushik & Cuervo, 2015). Misfolded proteins are either refolded, degraded, or sequestered to distinct cellular sites, such as aggresomes at the microtubule-organizing center, in a coordinated fashion (Johnston *et al*, 1998). When the proteostatic network becomes compromised during aging or stress conditions, aberrant proteins tend to accumulate as toxic aggregates, a process associated with numerous neurodegenerative diseases and other disorders (Lim & Yue, 2015).

Mitochondria have their own genome (mtDNA), which encodes < 1% of the mitochondrial proteome. To maintain their vital functions for energy production, mitochondria require the import of nuclear DNA-encoded proteins via the TOM/TIM complexes, coordinated expression and integration of nuclear DNA- and mtDNA-encoded OXPHOS subunits (Ryan & Hoogenraad, 2007), and sophisticated quality control systems at both the protein and organellar levels. Mitochondria have their own independent protein quality control system, including their own chaperones and proteases, such as Lon and ClpXP in the mitochondrial matrix (Voos, 2009; Fischer *et al*, 2012). At the organellar level, functionally compromised mitochondria can be selectively removed by

1 State Key Laboratory of Membrane Biology, Institute of Zoology, Chinese Academy of Sciences, Beijing, China

2 National Laboratory of Biomacromolecules, CAS Center for Excellence in Biomacromolecules, Institute of Biophysics, Chinese Academy of Sciences, Beijing, China

3 College of Life Science and Technology, HuaZhong University of Science and Technology, Wuhan, Hubei, China

4 School of Life Sciences, Peking University, Beijing, China

5 College of Life Sciences, Nankai University, Tianjin, China

6 University of Chinese Academy of Sciences, Beijing, China

*Corresponding author. Tel: +86 10 64807329; E-mail: liulei@ioz.ac.cn

**Corresponding author. Tel: +86 10 64807321; E-mail: chenq@ioz.ac.cn

either ubiquitin- or receptor-mediated mitophagy to ensure mitochondrial quality (Youle & Narendra, 2011; Khaminets *et al.*, 2016). Defective mitochondrial quality control leads to the accumulation of dysfunctional mitochondria, an etiological factor commonly observed in aging and age-related disorders. Apparently, proteostatic impairment and mitochondrial dysfunction work in concert and reinforce each other under stress conditions or during aging (Ross *et al.*, 2015). However, the underlying mechanisms and the primary cause for age-related disorders remain ill-defined. In an effort to address the mechanism of p62 translocation toward mitochondria, we have found that FUNDC1, a previously described mitophagy receptor, interacts with the cytosolic chaperone protein HSC70 to organize cellular proteostasis when proteasome is inhibited. Despite this, excessive mitochondrial accumulation of unfolded proteins prior to the formation of mitochondrion-associated protein aggregates (MAPAs) impairs mitochondrial integrity and activates AMPK, leading to cellular senescence.

Results

FUNDC1 interacts with HSC70 and promotes the mitochondrial recruitment of the proteasomal clients

We have previously shown that FUNDC1 is a highly conserved mitochondrial membrane protein that harbors a LC3-interacting region (LIR) to directly interact with LC3 and to mediate hypoxia-induced mitophagy (Liu *et al.*, 2012a). Transient expression of FUNDC1 resulted in the mitochondrial localization of LC3 in a manner that depended on the LIR motif (Appendix Fig S1). Unexpectedly, it promoted mitochondrial recruitment of p62/SQSTM1, a

multifunctional protein which binds ubiquitin through its UBA domain (Ciani *et al.*, 2003; Pankiv *et al.*, 2007), in a LIR-independent manner (Fig 1A and Appendix Fig S2A). Additionally, a p62 mutant lacking the UBA domain was less robustly recruited to mitochondria than the full-length p62 in cells overexpressing FUNDC1 or FUNDC1- Δ LIR (compare Appendix Fig S2A and B), suggesting that ubiquitin-modified proteins may be responsible for such recruitment. Indeed, expression of FUNDC1 or FUNDC1- Δ LIR resulted in the mitochondrial recruitment of ubiquitinated proteins (Fig 1B). Immunoblotting analysis of mitochondria isolated from HeLa cells revealed that overexpression of FUNDC1 or FUNDC1- Δ LIR resulted in the mitochondrial accumulation and consequent global elevation of ubiquitinated proteins (Fig 1C). FUNDC1 or FUNDC1- Δ LIR overexpression also resulted in the mitochondrial accumulation of p62, although had no visible effect on the level of this protein in total cell extract and cytosolic fractions (Fig 1C), likely due to the high abundance of p62 in cells.

We speculated that FUNDC1 may interact with other molecules for such recruitments. Mass spectral analysis of the proteins co-precipitated with FUNDC1 revealed HSC70, a constitutively expressed cytosolic chaperone protein belonging to the HSP70 family (Liu *et al.*, 2012b), as a novel FUNDC1-interacting partner (Fig 1D). Co-IP assay further confirmed the interaction between FUNDC1 and HSC70 (Fig 1E and F). The interaction seems specific, as HSP70, an inducible member of the HSP70 family that shares 85% homology with HSC70 (Liu *et al.*, 2012b), has limited capacity to interact with FUNDC1 (Fig 1G). In cells transiently expressing FUNDC1 or FUNDC1- Δ LIR, HSC70 was recruited to the mitochondria (Fig 1H). Fractionation analysis also revealed that overexpression of FUNDC1 resulted in the mitochondrial recruitment of HSC70 (Fig 1I).

Figure 1. FUNDC1 interacts with HSC70 and promotes the mitochondrial recruitment of the proteasomal clients.

- A HeLa cells were co-transfected with Myc empty vector (Myc), Myc-tagged FUNDC1 (F1-Myc) or Myc-tagged FUNDC1- Δ LIR mutant (Δ LIR-Myc), and Mito-OM-cherry, which localizes to the mitochondrial outer membrane, and immunostained with fluorescent anti-p62 and anti-Myc antibodies. Scale bar = 10 μ m.
- B HeLa cells were co-transfected with Myc, F1-Myc or Δ LIR-Myc, and Mito-OM-cherry and immunostained with anti-ubiquitin (Ub) and anti-Myc antibodies. Scale bar = 10 μ m.
- C Fractionation analysis of HeLa cells transfected with Myc, F1-Myc, or Δ LIR-Myc. The loading controls (LC) were α -tubulin for total cell lysate (TCL) and cytosolic fraction (Cyto), and HSP60 for mitochondrial fraction (Mito).
- D HeLa cells transfected with Myc or Myc/His6 double-tagged F1-Myc-His were lysed and precipitated with Ni-NTA beads. Samples were then subjected to SDS-PAGE. The differential band (upper arrow) was isolated and subjected to mass spectral analysis. The identified proteins with a score higher than 50 are listed.
- E Co-IP of endogenous HSC70 with F1-Myc or Δ LIR-Myc. α -Myc, anti-Myc antibody.
- F Co-IP of HSC70 with FUNDC1. α -F1, anti-FUNDC1 antibody. rIgG, control rabbit IgG.
- G Co-IP analysis of endogenous FUNDC1 with Flag-HSP70 or Flag-HSC70. α -Flag, anti-Flag antibody. Flag, empty vector.
- H HeLa cells were co-transfected with Myc, F1-Myc or Δ LIR-Myc, and Mito-OM-cherry and immunostained with anti-HSC70 and anti-Myc antibodies. Scale bar = 10 μ m.
- I Fractionation analysis of HeLa cells transfected with Myc or F1-Myc.
- J HeLa cells were co-transfected with Ub-R-GFP and Myc or F1-Myc and immunostained with fluorescent anti-Myc and anti-GFP (α -GFP) antibodies. The α -GFP signals in F1-Myc-transfected cells were lowered to avoid the overexposure of the mitochondrially localized R-GFP, making such signals of the equally distributed R-GFP invisible. Green arrowheads show the mitochondrially localized R-GFP proteins, which were more abundant than the equally distributed R-GFP and showed stronger R-GFP fluorescence, and white arrowheads show the mitochondrially localized R-GFP proteins without stronger R-GFP fluorescence, although abundant. Scale bar = 10 μ m.
- K Fractionation analysis of HeLa cells co-transfected with Ub-R-GFP and Myc or F1-Myc.
- L HeLa cells were co-transfected with Ub-R-GFP and F1-Myc. Mitochondria were isolated and then treated with or without proteinase K (Pro. K), or proteinase K in combination with digitonin or Triton X-100 (TX-100). Samples were then subjected to immunoblot analysis. HSP60, TIM23, and TOM20 are representatives of mitochondrial matrix-, mitochondrial inner membrane-, and mitochondrial outer membrane-localized proteins, respectively.
- M Fractionation analysis of HeLa cells stably transfected with control (Ctrl) shRNA vector or HSC70 shRNA and transiently co-transfected with Ub-R-GFP, Flag or Flag-HSC70 (shRNA-resistant), and Myc, or F1-Myc, as indicated.

Data information: In panels (C and I), three replicates were analyzed using Student's two-tailed *t*-test and are presented as the means \pm SEM. **P* < 0.05; ***P* < 0.01; NS, non-significant.

Source data are available online for this figure.

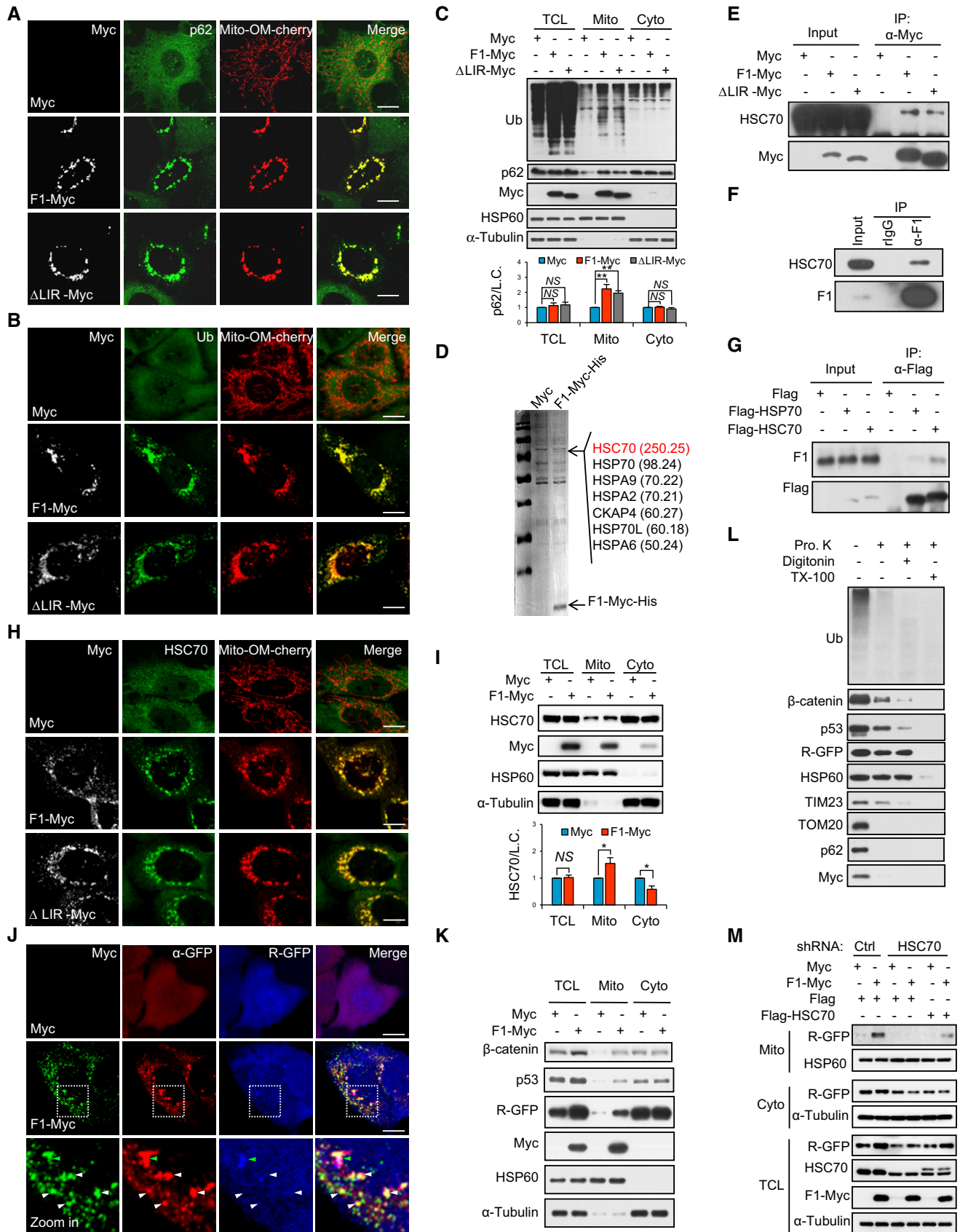


Figure 1.

CHIP is an HSC70-interacting E3 ubiquitin ligase which promotes the ubiquitination and subsequent proteasomal degradation of HSC70 clients (Connell *et al*, 2001). Confocal analysis revealed that CHIP was also recruited to mitochondria in response to FUNDC1 or FUNDC1- Δ LIR overexpression (Fig EV1A). Knockdown of either HSC70 or CHIP diminished the FUNDC1-induced mitochondrial localization of ubiquitin and p62 (Appendix Figs S3 and S4). These data suggest that overexpressed FUNDC1 may recruit HSC70 and its unfolded clients, including proteasomal substrates, to mitochondria; the client proteins are then subjected to ubiquitination by CHIP and hence endowed with the ability to attract p62.

To prove this, Ub-R-GFP, a GFP-based reporter for proteasomal degradation, was employed for the following study. The fused ubiquitin moiety of Ub-R-GFP will be cleaved in cells, producing an N-end rule substrate R-GFP (Dantuma *et al*, 2000). We found that R-GFP, but not stable GFP, can be recognized by HSC70, depending on the latter's peptide-binding domain (PBD; Fig EV1B and C), a region required for the binding of HSC70 clients (Fourie *et al*, 1994). Additionally, FUNDC1 overexpression resulted in the recruitment of R-GFP proteins to FUNDC1-labeled mitochondria as expected; these R-GFP proteins could be clearly visualized by immunostaining using anti-GFP-antibody, although some of their own fluorescence were undetectable (Figs 1J and EV1D), which is likely due to their aberrant conformation. Subcellular fractionation analysis also revealed that FUNDC1 overexpression resulted in the accumulation of the R-GFP proteins and p53 and β -catenin, two endogenous proteasomal substrates, in mitochondria (Fig 1K). Proteinase K protection assays showed that the mitochondrially recruited R-GFP, β -catenin, and p53 proteins showed a certain degree of resistance to digestion even when treated with digitonin, which permeabilizes the outer membrane of mitochondria, but not when treated with Triton X-100, which permeabilizes both outer and inner mitochondrial membranes (Fig 1L). This indicates that a portion of the recruited client proteins were imported into the mitochondrial matrix. The mitochondrially recruited p62 and ubiquitinated proteins, however, showed hardly any resistance to proteinase K digestion (Fig 1L),

suggesting that most of these proteins were on the surface of mitochondria. Additionally, we found that FUNDC1-induced mitochondrial recruitment of R-GFP was diminished in HSC70-knockdown cells and was partially restored by reintroduction of shRNA-resistant Flag-HSC70 (Figs 1M, and EV1E and F). CHIP knockdown, however, had no obvious effect on the mitochondrial recruitment of R-GFP caused by FUNDC1 overexpression (Fig EV1E and F). These data suggest that HSC70 may reroute its client proteins from fast proteasomal degradation to mitochondria via interaction with the overexpressed FUNDC1.

FUNDC1 and HSC70 are required for the translocation of unfolded cytosolic proteins to mitochondria in proteasome-inhibited cells

Given the critical role of HSC70 in recognition of cytosolic unwanted proteins, we hypothesized that the interaction between FUNDC1 and HSC70 may be the missing link between mitochondrial and cytosolic proteostasis network. We thus checked whether the cytosolic proteasomal clients could be recruited to mitochondria in a FUNDC1-/HSC70-dependent fashion under proteostatic stress conditions. In R-GFP-expressing cells treated with the proteasome inhibitor MG132, the accumulation of R-GFP proteins could be visualized by immunostaining using anti-GFP antibody (Fig EV2A, upper rows). The mitochondrially recruited R-GFP proteins were discernible only when the cytosolic proteins were extracted by digitonin (Fig EV2A, lower rows), but their own fluorescence was undetectable. Fractionation analysis also revealed that R-GFP, p53, and β -catenin proteins were recruited to mitochondria in the presence of the proteasome inhibitors MG132 or lactacystin (Figs 2A and EV2B). Proteinase K protection assays showed that most of the R-GFP and some of p53 and β -catenin proteins that were recruited to mitochondria were imported into the mitochondrial matrix (Fig 2B). The mitochondrially localized R-GFP proteins isolated from TOM20-, TOM22-, and TOM70-knockdown cells were much less resistant to proteinase digestion compared to those isolated

Figure 2. FUNDC1/HSC70 interaction is required for the mitochondrial translocation of proteasomal clients under stress conditions.

- A Fractionation analysis of the HeLa cells transfected with Ub-R-GFP and treated with DMSO (control vehicle) or 10 μ M MG132 for 4 h.
- B Proteinase K protection analysis of the mitochondria isolated from the HeLa cells transfected with Ub-R-GFP and treated with MG132.
- C Proteinase K protection analysis of the mitochondria isolated from HeLa cells co-transfected with Ub-R-GFP and Ctrl, TOM20, TOM22, or TOM70 shRNA and treated with MG132.
- D Fractionation analysis of HeLa cells stably transfected with Ctrl or LONP1 shRNA and transiently co-transfected with Ub-R-GFP and Myc or LONP1 (shRNA-resistant) and then treated with DMSO or MG132.
- E Fractionation analysis of HeLa cells stably transfected with Ctrl shRNA, F1 shRNA, or F1 shRNA together with shRNA-resistant F1-Myc or Δ LIR-Myc, and transiently transfected with Ub-R-GFP and then treated with DMSO or MG132.
- F Fractionation analysis of HeLa cells stably transfected with Ctrl or HSC70 shRNA and transiently co-transfected with Ub-R-GFP and Flag or shRNA-resistant Flag-HSC70 and then treated with DMSO or MG132.
- G Fractionation analysis of HeLa cells stably transfected with Ctrl or HSP70 shRNA and transiently co-transfected with Ub-R-GFP and Flag or shRNA-resistant Flag-HSP70 and then treated with DMSO or MG132.
- H Mitochondria were isolated from the untransfected cells, cytosols were isolated from the cells transfected with GFP or Ub-R-GFP and treated with DMSO or MG132 for 8 h, and the isolated mitochondria and cytosols were then subjected to *in vitro* protein import analysis.
- I Mitochondria isolated from the untransfected cells were resuspended in the cytosol isolated from the cells transfected with Ub-R-GFP and incubated at RT for 1 hour, and the mitochondria were then isolated from the *in vitro* system and then treated with or without proteinase K and subjected to immunoblot analysis.
- J Mitochondria were isolated from the cells transfected with Ctrl shRNA, F1 shRNA, or F1 shRNA together with F1-Myc, cytosols were isolated from the cells transfected with Ub-R-GFP, and the isolated mitochondria and cytosols were then subjected to *in vitro* protein import analysis.
- K Cytosol isolated from the cells transfected with Ub-R-GFP was mixed with the cytosols isolated from the cells transfected with Ctrl shRNA, HSC70 shRNA, or HSC70 shRNA together with Flag-HSC70, mitochondria were isolated from the untransfected cells, and the isolated mitochondria and cytosol mixtures were then subjected to *in vitro* protein import analysis.

Source data are available online for this figure.

from control cells (Figs 2C and EV2C), suggesting that TOM complex is required for the import of the proteasomal clients into mitochondria. The mitochondrial accumulation of R-GFP upon MG132 treatment was augmented in the LONP1-knockdown cells, and this was reversed by reintroduction of shRNA-resistant LONP1 (Figs 2D and EV2D), suggesting that LONP1 may degrade the proteasomal clients imported into the mitochondrial matrix. These results are in agreement with the findings in yeast (Ruan *et al*, 2017).

We next addressed the question of whether FUNDC1 and HSC70 are required for the mitochondrial translocation of the proteasomal clients. First, we found that the MG132-induced mitochondrial accumulation of R-GFP was reduced in FUNDC1-knockdown or FUNDC1-knockout cells (Figs 2E, and EV2E and F). Reintroduction of shRNA-resistant FUNDC1 or FUNDC1-ΔLIR in FUNDC1-knockdown cells restored the mitochondrial accumulation of R-GFP (Figs 2E and EV2E). HSC70 knockdown also diminished the MG132-induced mitochondrial translocation of R-GFP, which

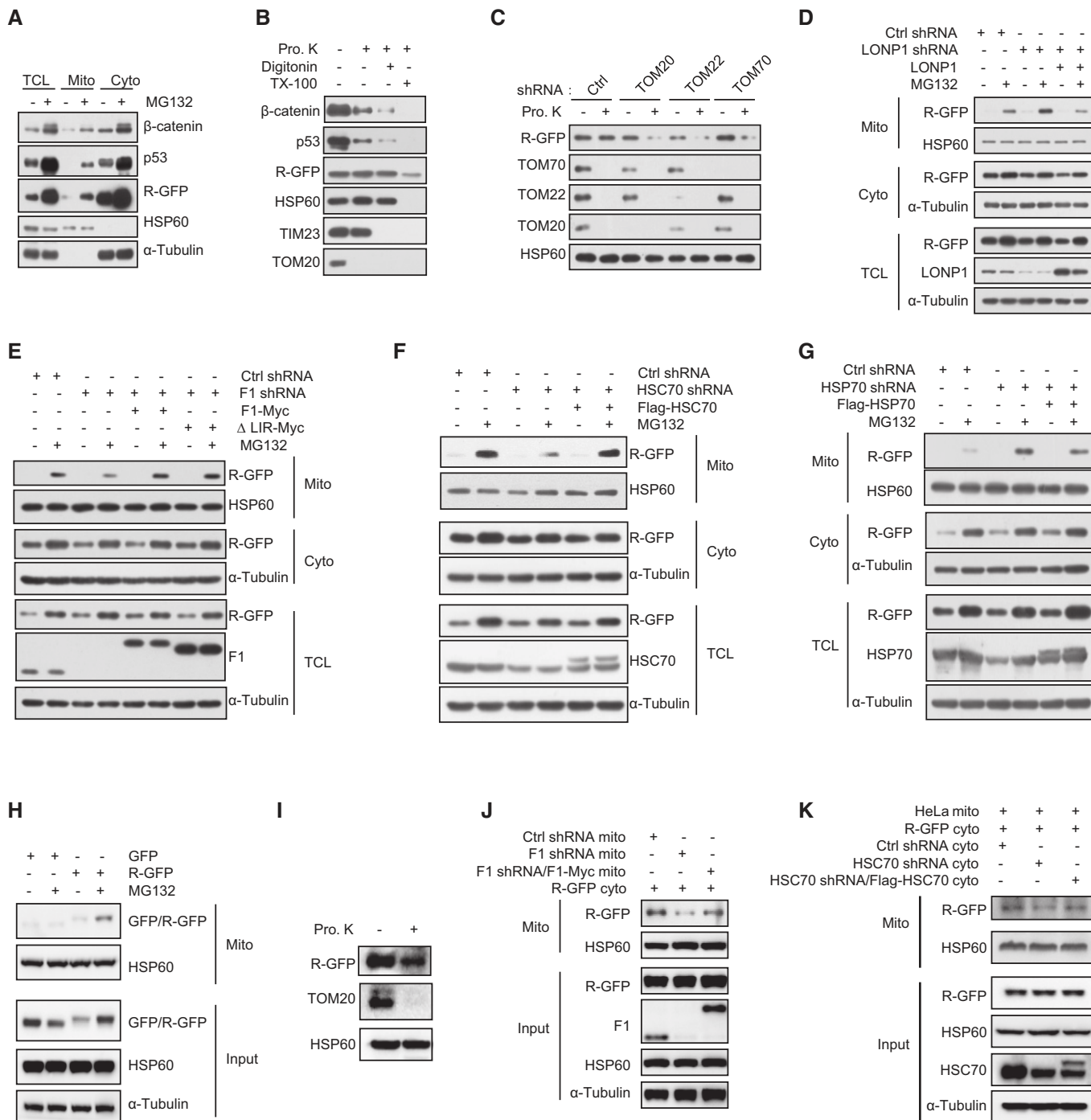


Figure 2.

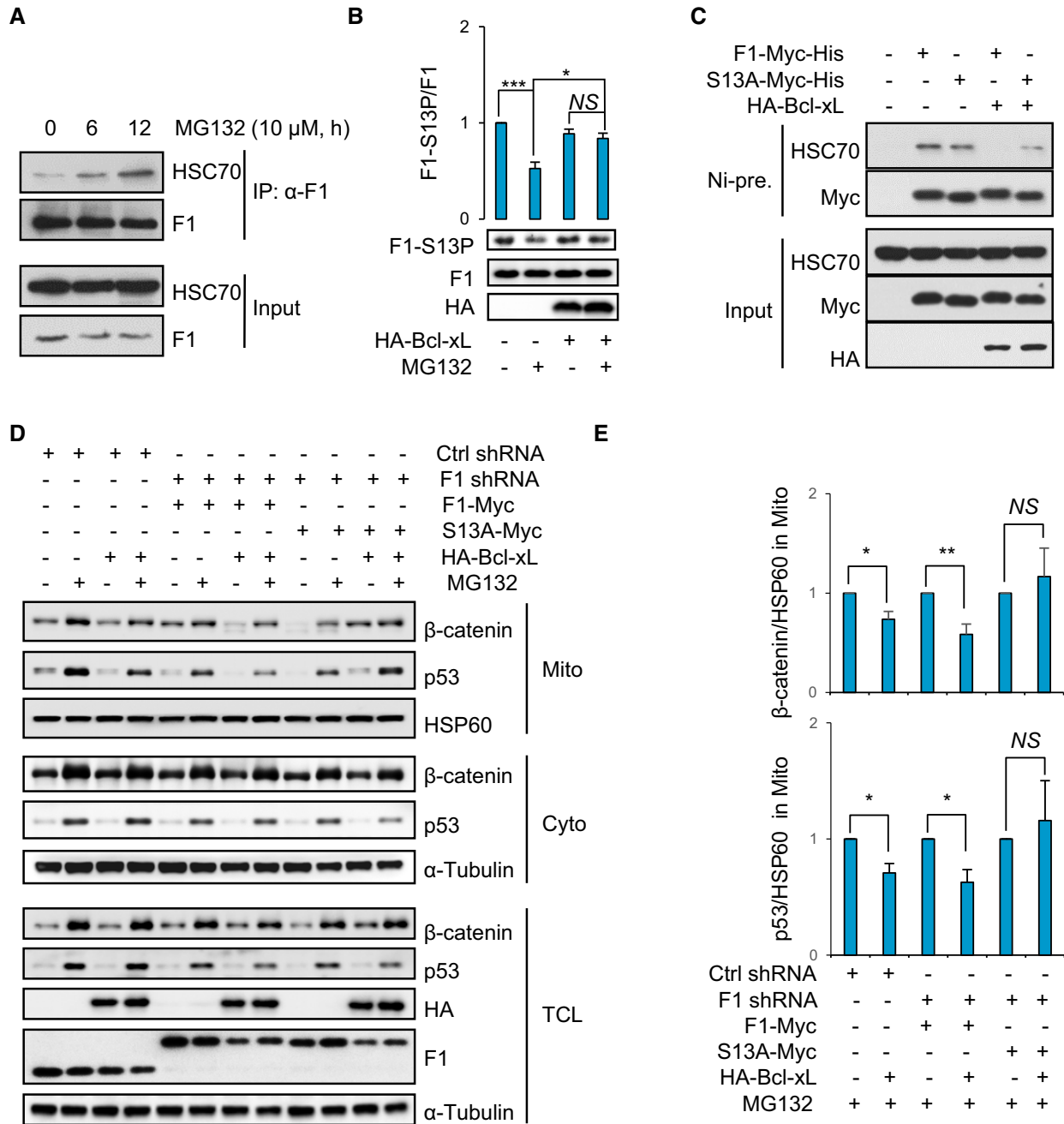


Figure 3. Bcl-xL regulates the interaction between FUNDC1 and HSC70.

A Co-IP of HSC70 with FUNDC1 in HeLa cells treated with MG132 as indicated.

B Immunoblot analysis of the HeLa cells transfected with or without HA-Bcl-xL and treated with DMSO or MG132 for 6 h.

C Ni²⁺-NTA precipitation of HeLa cells transfected with indicated vectors. S13A-Myc-His, Myc/His6 double-tagged FUNDC1-S13A mutant.

D, E Fractionation analysis of HeLa cells transfected with indicated vectors and treated with DMSO or MG132. Quantification is shown in (E).

Data information: In panels (B and E), three replicates were analyzed using Student's two-tailed t-test and are presented as the means ± SEM. **P* < 0.05; ***P* < 0.01; ****P* < 0.001; NS, non-significant.

Source data are available online for this figure.

was partially restored by expression of shRNA-resistant Flag-HSC70 (Figs 2F and EV2G). In contrast, HSP70 knockdown aggravated the MG132-induced mitochondrial translocation of R-GFP, and this was counteracted by expression of shRNA-resistant

Flag-HSP70 (Figs 2G and EV2H). These data suggest that both FUNDC1 and HSC70 are required for the mitochondrial recruitment of proteasomal clients. HSP70, however, may prevent such recruitment.

Figure 4. Effects of FUNDC1, HSC70, HSP70, TOM complex, Bcl-xL, and LONP1 on the formation of MAPAs in response to proteasome inhibition.

- A HeLa cells were transfected with GFP-p62, treated with DMSO or 10 μ M MG132 for 8 h, and then immunostained with anti-Ub and anti- γ -tubulin antibodies. Note that the aggresome (blue arrowhead), rather than the MAPAs (white arrowheads), colocalizes with γ -tubulin. Scale bar = 10 μ m.
- B, C HeLa cells were stably transfected with the indicated vectors, treated with MG132, and immunostained with the indicated antibodies. Scale bar = 10 μ m. Quantification is shown in (C).
- D, E HeLa cells were transfected with Ctrl, TOM20, TOM22, or TOM70 shRNA vectors including nuclear localized GFP (N-GFP) expressing elements and then treated with MG132 and immunostained with the indicated antibodies. Scale bar = 10 μ m. Quantification is shown in (E).
- F, G HeLa cells were transfected with GFP or GFP-Bcl-xL and then treated with MG132 and immunostained with anti-p62 antibodies. Scale bar = 10 μ m. Quantification is shown in (G).
- H, I HeLa cells were stably transfected with Ctrl or LONP1 shRNA, treated with MG132, and immunostained with the indicated antibodies. Scale bar = 10 μ m. Quantification is shown in (I).

Data information: In panels (C, E, G and I) three replicates were analyzed using Student's two-tailed *t*-test and are presented as the means \pm SEM. **P* < 0.05; ***P* < 0.01; ****P* < 0.001.

To further substantiate our finding that FUNDC1 interacts with HSC70 to recruit proteasomal clients to mitochondria, we used an *in vitro* assay in which we incubated the mitochondria isolated from untransfected cells with the cytosol isolated from cells expressing R-GFP or GFP (Fig EV2I). More R-GFP proteins were recruited to mitochondria compared to stable GFP proteins and were imported into mitochondria as judged by their resistance to protease digestion (Fig 2H and I). As expected, both FUNDC1 and HSC70 were required for the mitochondrial recruitment of R-GFP even in this *in vitro* system (Figs 2J and K, and EV2J and K).

These results collectively suggested that in response to proteostatic stress, HSC70 may take its clients via interaction with FUNDC1 to mitochondria for import and degradation by LONP1. Additionally, we propose that HSC70 and HSP70 may partition their clients to different pathways for complementary degradation.

Bcl-xL regulates the interaction between FUNDC1 and HSC70

We found that the interaction between FUNDC1 and HSC70 was increased in the proteasome-inhibited cells (Fig 3A). Meanwhile, FUNDC1 was dephosphorylated at serine 13 (Ser13), which was suppressed by Bcl-xL expression (Fig 3B), consistent with previous report (Chen *et al*, 2014; Wu *et al*, 2014). Interestingly, we found that Bcl-xL expression suppressed the interaction of HSC70 with FUNDC1, while had no notable effect on that with FUNDC1-S13A mutant (Fig 3C), suggesting that Bcl-xL may regulate the FUNDC1/HSC70 interaction through modulating the phosphorylation status of FUNDC1 at Ser13. We next checked the effect of Bcl-xL on the mitochondrial recruitment of unfolded cytosolic proteins and found that Bcl-xL suppressed the MG132-induced mitochondrial translocation of representative proteasomal clients in control cells and in FUNDC1-knockdown cells reintroduced with wild-type FUNDC1, while not in the FUNDC1-knockdown cells reintroduced with FUNDC1-S13A (Fig 3D and E). These data suggest that the FUNDC1/HSC70 interaction, which is regulated by the phosphorylation status of FUNDC1 at Ser13, is required for the mitochondrial recruitment of proteasomal clients under stress conditions.

FUNDC1 and HSC70 are required for the formation of MAPAs in response to proteasome inhibition

Overwhelming evidence has shown that proteostatic stress causes protein aggregation, leading to the formation of aggresomes at the microtubule-organizing center region (Hyttinen *et al*, 2014). In

HeLa, U2OS, and HepG2 cells, proteasome inhibition resulted in the formation of both aggresomes (colocalized with the centrosome marker γ -tubulin) and large amounts of other protein aggregates that are positive for ubiquitin and p62 (Figs 4A and EV3A–C). We named these non-aggresome aggregates as mitochondrion-associated protein aggregates (MAPAs), given the organizing role of mitochondria in their formation and the incorporation of mitochondrial proteins into them (see below). Knockdown or knockout of FUNDC1 had no obvious effect on the MG132-induced formation of aggresomes, while abrogated the formation of MAPAs (Figs 4B and C, and EV3D and E). Reintroduction of either FUNDC1 or FUNDC1- Δ LIR in FUNDC1-knockdown cells restored the MAPA formation (Fig 4B and C). HSC70 knockdown also abrogated the formation of MAPAs (Fig 4B and C). In contrast, HSP70 knockdown enhanced the formation of MAPAs (Fig 4B and C). Additionally, MG132-induced MAPAs were decreased in Bcl-xL-expressed cells or in TOM20-, TOM22- or TOM70-knockdown cells, while increased in LONP1-knockdown cells (Fig 4D–I). The effects of these molecules on the MAPA formation were highly correlated with their effects on the mitochondrial translocation or accumulation of the proteasomal clients, indicating that the mitochondrial recruitment of the proteasomal clients is important for triggering the formation of MAPAs. FUNDC1 and HSC70 therefore may promote the MAPA formation by mediating the mitochondrial translocation of proteasomal clients.

Mitochondrial proteins are incorporated into the MAPAs

To investigate the properties of MAPAs in more detail, we first employed the cryogenic super-resolution correlative light and electron microscopy (csCLEM) assay (Liu *et al*, 2015). It was shown that the GFP-p62-labeled MAPA we observed under light microscope contained some layered structures (Fig 5A). Transmission electron microscopy (TEM) analysis further showed that proteasome inhibition resulted in the appearance of the layered structures inside mitochondria or in close proximity to mitochondria, in addition to their existences in MAPAs (Fig 5B). We thus speculated that MAPAs may originate from mitochondria, or at least, mitochondrial components may constitute MAPAs. To test this, we took advantage of the fact that protein aggregates are insoluble in TX-100 (Lystad & Simonsen, 2015). When cells were treated with MG132, R-GFP and ubiquitinated proteins accumulated in both TX-100-soluble and TX-100-insoluble fractions (Fig 5C and D). Interestingly, p62 and FUNDC1 were decreased in the TX-100-soluble fractions and increased in the insoluble fractions (Fig 5C and D, and Appendix Fig S5A). Some

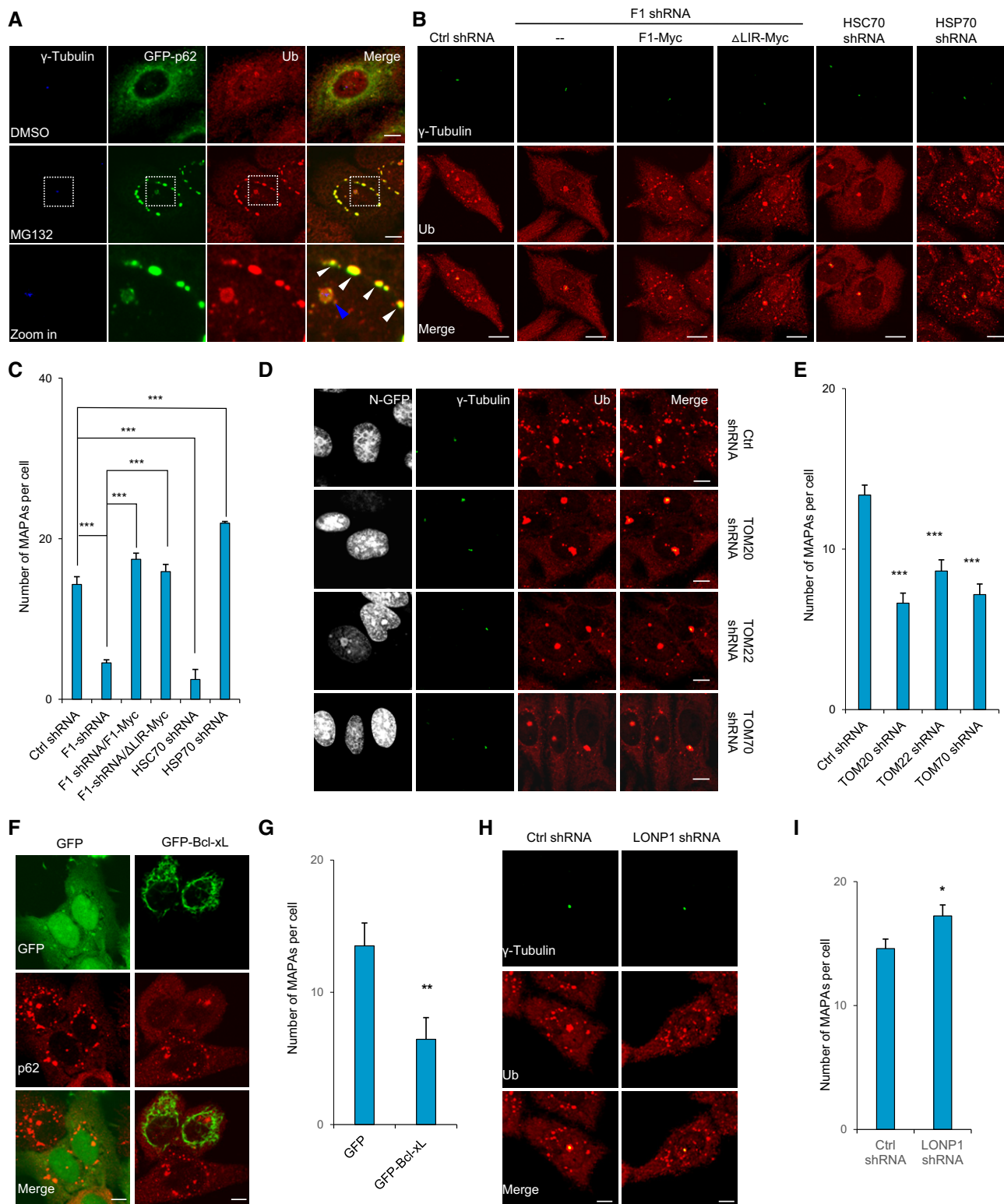


Figure 4.

other mitochondrial membrane proteins (TOM70, TIM23, and TOM20) showed similar patterns of deposition (Fig 5C and Appendix Fig S5A). The mitochondrial matrix protein (HSP60 and LONP1) and marker proteins of the ER (calnexin and calreticulin),

golgi (GOLM1 and GM130), and lysosome (LAMP2), however, showed no increased deposition in the TX-100-insoluble fractions (Fig 5C and Appendix Fig S5A). We next found that the mitochondrial outer membrane-localized Mito-OM-GFP, but not diffuse

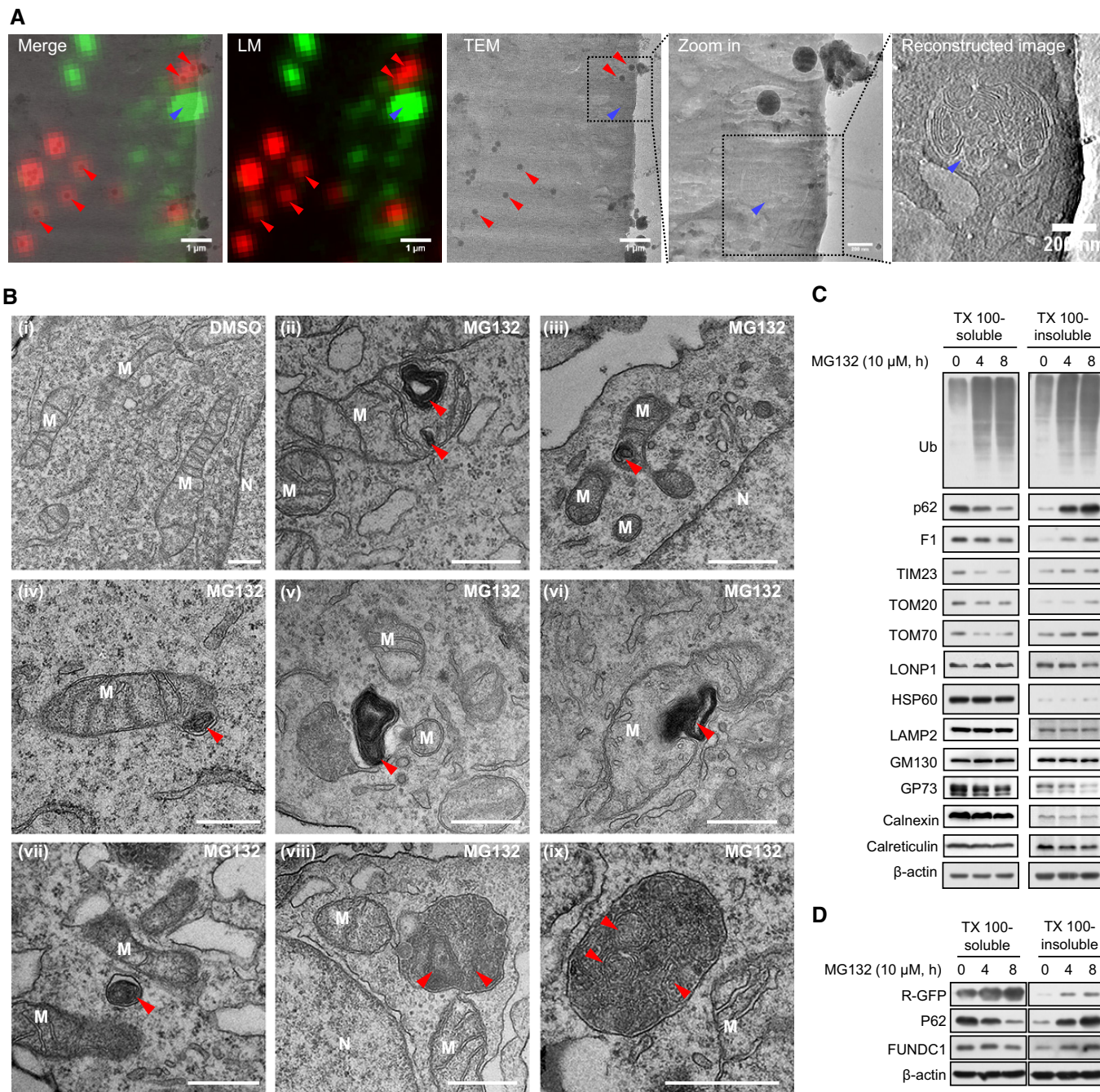


Figure 5. MAPAs contain layered structures and mitochondrial proteins.

A cSLEM analysis of cells transfected with GFP-p62 and treated with MG132. Red arrowheads show the dark red fluorescent beads used to correlate the images from light microscopy (LM) and transmission electron microscopy (TEM). The blue arrowhead shows a MAPA observed under LM and TEM.

B TEM analysis of HeLa cells treated with DMSO or MG132. Note the layered structures (red arrowheads) in the mitochondrial matrix (ii, iii), budding from mitochondria (iv), attached to mitochondria (v, vi), away from mitochondria (vii), or inside the MAPAs (viii, ix) in MG132-treated cells. Scale bar = 500 nm. M, mitochondrion. N, nucleus.

C Immunoblot analysis of the TX-100-soluble and TX-100-insoluble fractions of HeLa cells treated with MG132 as indicated.

D Immunoblot analysis of the TX-100-soluble and TX-100-insoluble fractions of HeLa cells transfected with Ub-R-GFP and treated with MG132 as indicated.

Source data are available online for this figure.

cytosolic GFP or mitochondrial matrix-localized Mito-MTX-GFP, were increased in the TX-100-insoluble fractions in MG132-treated cells (Appendix Fig S5B), suggesting that the mitochondrial

membrane-localized proteins are more prone to deposit in response to proteasome inhibition. As expected, MG132-induced deposition of mitochondrial membrane proteins was positively regulated by

FUNDC1, HSC70, and TOM complex, and was negatively regulated by Bcl-xL, HSP70, and LONP1 (Fig EV4A–F and Appendix Fig S5C), consistent with the effects of these molecules on MAPA formation.

In line with the deposition of mitochondrial membrane proteins upon proteasome inhibition, we observed the colocalization of p62-labeled MAPAs with Mito-OM-cherry, TIM23, and overexpressed FUNDC1, but not with Mito-MTX-GFP (Fig 6A and B, and Appendix Fig S6). These data collectively suggested that the deposited mitochondrial membrane proteins were incorporated into the MAPAs.

We next asked whether the unfolded proteins in the mitochondrial matrix were incorporated into the MAPAs. We expressed the unfolding-prone protein OTC- Δ (Zhao *et al*, 2002) in the mitochondrial matrix and found that it colocalized with MAPAs in MG132-treated cells, while wild-type OTC remained in the mitochondrial matrix (Figs 6C and EV4G), suggesting that within the mitochondrial matrix, unfolded proteins, but not correctly folded ones, are incorporated into MAPAs.

To corroborate these findings, we employed the Apex (ascorbate peroxidase) technique, which is widely used for subcellular imaging of specific proteins by electron microscopy (EM). We transfected cells with OTC- Δ -Apex or mitochondrial outer membrane-localized Mito-OM-Apex and then treated these cells with MG132 followed by DAB staining and TEM analysis. OTC- Δ was concentrated in certain region of mitochondrial matrix (Fig 6D), consistent with the confocal analysis (Figs 6C and EV4G). Both OTC- Δ -Apex and Mito-OM-Apex signals were inside the MAPAs (Fig 6D), confirming that the mitochondrial membrane-localized proteins and mitochondrial matrix-localized misfolded proteins are incorporated into the MAPAs.

FIS1 is required for the formation of MAPAs

Using time-lapse imaging, we observed the segregation of OTC- Δ -GFP-positive Mito-MTX-DsRed-negative structures from the mitochondrial network (Fig 7A), suggesting a potential role of the mitochondrial fission machinery in MAPA formation. To prove this, we developed DLP1- and FIS1-knockdown cells and found that DLP1 knockdown had no visible effect on the MG132-induced deposition of p62, TIM23, and FUNDC1 in the Triton X-100-insoluble fractions (Fig 7B). While, knockdown of FIS1 diminished the deposition of FUNDC1, and this was reversed by the reintroduction of shRNA-resistant Flag-FIS1 (Fig 7C and D). In line with this, MG132-induced MAPAs were decreased in FIS1-knockdown cells (Fig 7E and F). The reduction in MAPA formation caused by FIS1 deficiency may result in the mitochondrial retention of the client proteins recruited to this

organelle, as FIS1 knockdown augmented the MG132-induced mitochondrial accumulation of R-GFP, an effect which was reversed by the reintroduction of Flag-FIS1 (Fig 7G and H). It should be noted that the accumulation of misfolded proteins in the mitochondrial matrix itself is required, but not sufficient to trigger MAPA formation (Figs 4D, E, H, I and 6C, and EV4G), and the MAPAs consist of p62 and ubiquitinated proteins in addition to mitochondrial components. We thus propose that the unfolded cytosolic proteins imported into mitochondria, if not degraded by LONP1, may concentrate in certain regions and then become segregated from the mitochondria in a FIS1-dependent manner in response to proteostatic stress. The segregated mitochondrial components may combine with ubiquitinated proteins and p62 at the outer membrane of mitochondria to form MAPAs, although the precise mechanism of MAPA formation requires further investigation.

FUNDC1 is required for the autophagic degradation of MAPAs

The autophagy pathway is activated to degrade protein aggregates when proteasome activity is inhibited (Pandey *et al*, 2007). In line with this, the autophagosome marker LC3 colocalized with MAPAs as revealed by confocal analysis (Fig 8A) and by Apex-LC3 analysis (Fig 6D). Most of the MAPAs were enclosed by membranes, resembling the amphisomes/autolysosomes, a structure representing that autophagosome is fused with endosomes/lysosomes (Mizushima *et al*, 2010). Immunoblotting analysis revealed that proteasome inhibition resulted in the activation of autophagy (LC3-II up-regulation) and decline of representative mitochondrial membrane proteins (TIM23 and TOM20) and p62, while had marginal effect on the levels of representative mitochondrial matrix proteins (HSP60 and LONP1; Figs 8B and EV5A). Depletion of autophagy-related ATG5 abrogated MG132-induced autophagy, prevented the decline of p62 and representative mitochondrial membrane proteins, and enhanced the accumulation of R-GFP (Figs 8C and E, and EV5B). These data collectively suggest that autophagy is responsible for the degradation of MAPAs, which consist of p62, proteasomal clients, and mitochondrial membrane proteins, and devoid of mitochondrial matrix-localized correctly folded proteins.

Interestingly, we found that FUNDC1 knockdown also prevented the MG132-induced decline of representative mitochondrial membrane proteins and enhanced the accumulation of R-GFP (Figs 8D and E, and EV5C), and these effects were reversed by reintroduction of FUNDC1, but not FUNDC1- Δ LIR (Figs 8D and E, and EV5C). Additionally, we found that the MAPAs formed in FUNDC1-knockdown cells reintroduced with FUNDC1- Δ LIR were devoid of GFP-LC3, while the MAPAs formed in the control and

Figure 6. Mitochondrial proteins are selectively incorporated into MAPAs.

- HeLa cells were co-transfected with Mito-OM-cherry and Mito-MTX-GFP and then treated with DMSO or MG132 and immunostained with anti-p62 antibody. Note the colocalization of a p62 punctum with a structure that is positive for Mito-OM-cherry but not for Mito-MTX-GFP (white arrowheads) in MG132-treated cells. Scale bar = 10 μ m.
- HeLa cells were transfected with Mito-MTX-GFP and then treated with DMSO or MG132 and immunostained with anti-p62 and anti-TIM23 antibodies. Note the colocalization of a p62 punctum with a structure that is positive for TIM23 but not for Mito-MTX-GFP (white arrowhead) in MG132-treated cells. Scale bar = 10 μ m.
- HeLa cells were co-transfected with Mito-MTX-GFP and OTC-Myc or OTC- Δ -Myc, treated with DMSO or MG132, and immunostained with anti-Myc and anti-p62 antibodies. Note that the p62-labeled MAPAs were colocalized with OTC- Δ (red arrowheads), but not with OTC (white arrowheads) in the MG132 treated cells. Scale bar = 10 μ m.
- TEM analysis of HeLa cells transfected with indicated vectors, treated with MG132, and stained with DAB. Blue arrowheads show MAPAs, and red arrowheads show electron-dense Apex signals. Scale bar = 500 nm. M, mitochondrion.

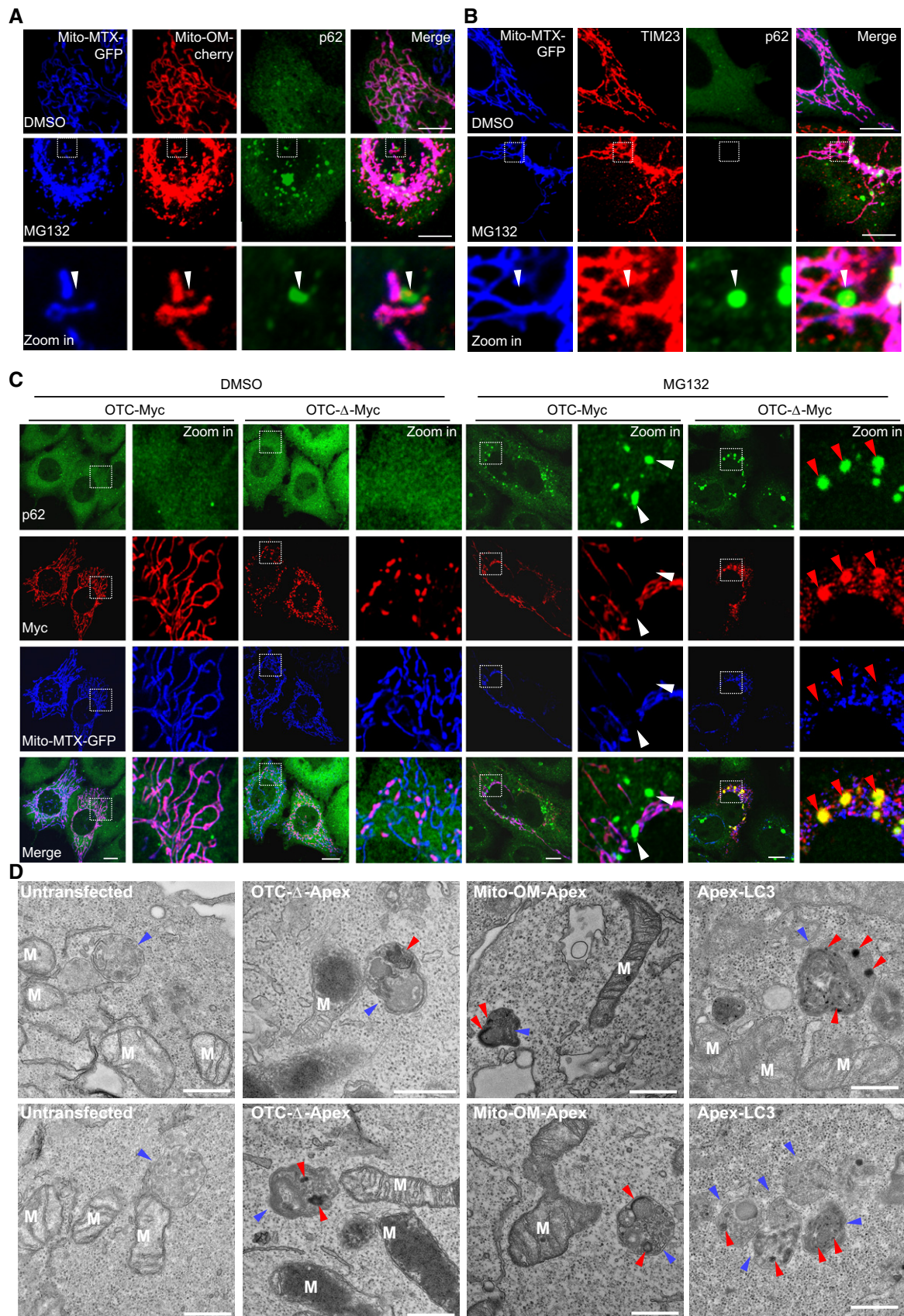


Figure 6.

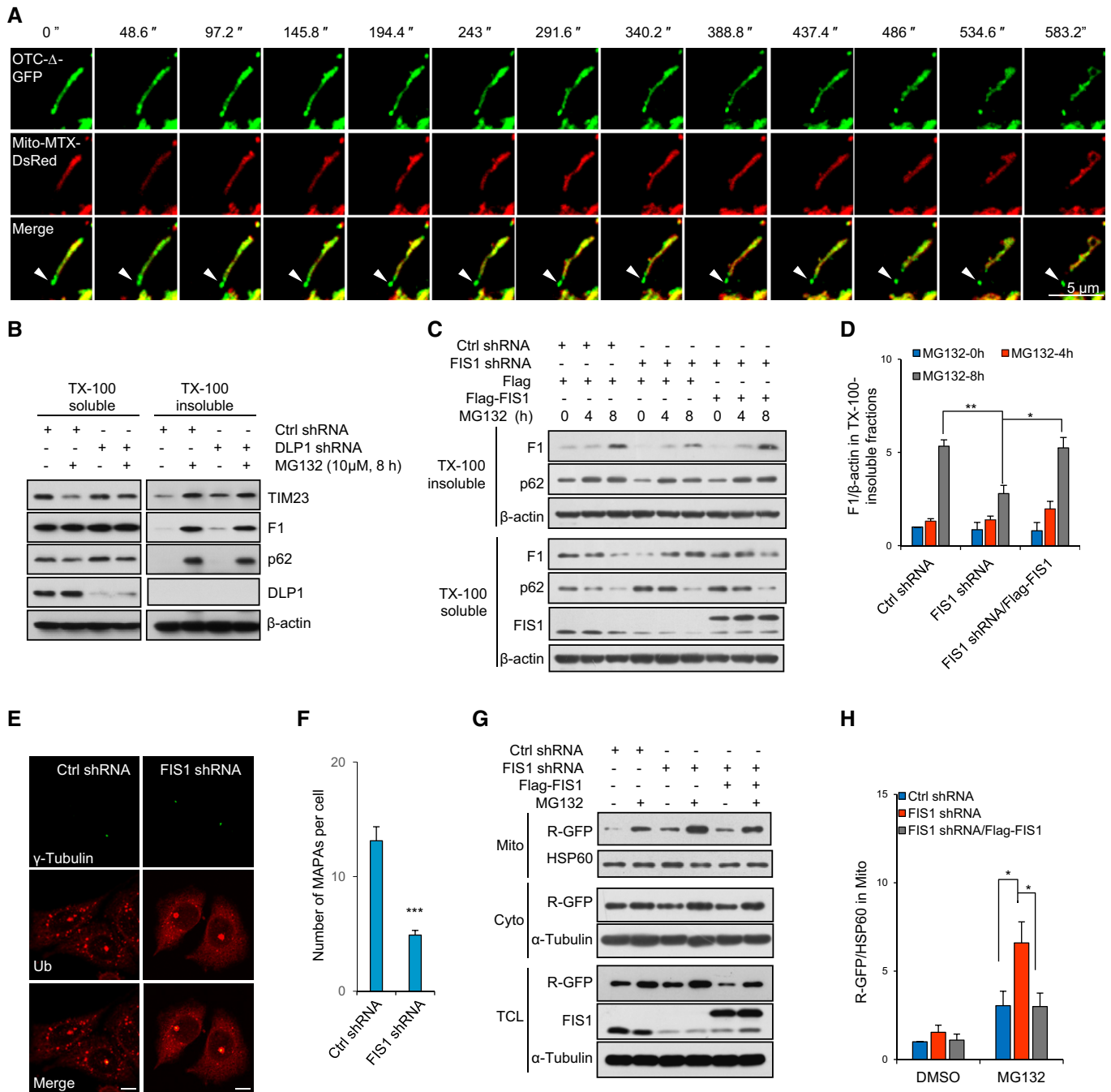


Figure 7. FIS1 is required for the formation of MAPAs.

A Time-lapse analysis of live HeLa cells transfected with OTC-Δ-GFP and Mito-MTX-DsRed and treated with MG132. White arrowheads show a OTC-Δ-GFP-positive Mito-MTX-DsRed-negative structure that eventually segregated from the mitochondrial network.

B Immunoblot analysis of the MG132-induced deposition of FUNDC1, TIM23, and p62 in HeLa cells transfected with Ctrl or DLP1 shRNA.

C, D Immunoblot analysis of the MG132-induced deposition of FUNDC1 in cells transfected with Ctrl shRNA, FIS1 shRNA, or FIS1 shRNA together with shRNA-resistant Flag-FIS1. Quantification is shown in (D).

E, F HeLa cells were stably transfected with Ctrl or FIS1 shRNA, treated with MG132, and immunostained with indicated antibodies. Scale bar = 10 μm. Quantification is shown in (F).

G, H Fractionation analysis of HeLa cells stably transfected with Ctrl or FIS1 shRNA and then transiently co-transfected with Ub-R-GFP and Flag or Flag-FIS1 and treated with DMSO or MG132. Quantification is shown in (H).

Data information: In panels (D, F and H), three replicates were analyzed using Student's two-tailed *t*-test and are presented as the means ± SEM. **P* < 0.05; ***P* < 0.01; ****P* < 0.001.

Source data are available online for this figure.

FUNDC1-knockdown cells reintroduced with wild-type FUNDC1 were colocalized with GFP-LC3 puncta (Fig 8F). TEM analysis also showed that the MAPAs formed in the FUNDC1-knockdown cells reintroduced with FUNDC1- Δ LIR were exposed to the cytosol and devoid of intact amphisomal/autolysosomal membranes enclosing them (Fig 8G). These data are consistent with the results showing that overexpressed FUNDC1- Δ LIR recruited p62, but not GFP-LC3, to mitochondria (Fig 1A and Appendix Fig S1). Our results thus uncover a new role of FUNDC1 in promoting the degradation of MAPAs under proteotoxic stress conditions, in addition to its characterized role as a mitophagy receptor under hypoxic conditions (Liu *et al*, 2012a).

FUNDC1 and HSC70 are required for the proteotoxic stress-induced cellular senescence

It has been well documented that proteasome inhibition results in mitochondria dysfunction and cellular senescence in cultured cells (Ling *et al*, 2003; Chondrogianni & Gonos, 2004; Pei *et al*, 2004; Sullivan *et al*, 2004; Chondrogianni *et al*, 2008; Torres & Perez, 2008). To test the effect of FUNDC1-/HSC70-mediated pathway on cell fate, we established a model of senescence by treating HeLa cells with MG132 for 8 h and then incubating them in normal complete medium for a further 3 days. More than 20% of the cells displayed SA- β -gal-positive staining (Fig 9A and B). Immunoblotting analysis showed that the AMPK activity and the levels of oxidized proteins in MG132-pulse-treated cells were consistently higher than those in control cells until 3 days after treatment withdrawal (Fig 9C and D, and Appendix Fig S7A). Pulse treatment with MG132 also resulted in the up-regulation of the senescence markers p53 and p21, but not p16 (CDKN2A), at 24 h and until 3 days after treatment withdrawal (Fig 9C and D). The AMPK inhibitor Compound C (Fig 9E and F), but not the ROS scavengers MitoTEMPO and NAC (Appendix Fig S7B and C), prevented MG132-induced SA- β -gal-positive staining and up-regulation of p53 and p21, suggesting a potential role of AMPK in this process.

This senescent phenotype seems to depend on the mitochondrial accumulation of proteasomal client substrates. It was positively regulated by FUNDC1 and HSC70, and it was negatively regulated by Bcl-xL, HSP70, LONP1, and FIS1 (Fig 9G–P, Appendix Fig S7D and E). The effects of these molecules on cell senescence were highly correlated with their effects on the mitochondrial accumulation of proteasomal clients. In particular, it should be noted that FIS1 knockdown aggravated mitochondrial accumulation of proteasomal clients and cell senescence, although it abrogated MAPA

formation (Figs 7E–H, and 9O and P). Thus, mitochondrial accumulation of unfolded proteins, rather than MAPA formation, is probably responsible for the occurrence of cell senescence, in agreement with the fact that even monomeric aggregation-prone proteins are toxic to mitochondria and cells (Ganguly *et al*, 2017).

Discussion

In the present study, we have provided evidence to show that the FUNDC1/HSC70 interaction promotes the mitochondrial translocation of unfolded cytosolic proteins to mitochondria for degradation by LONP1 or for formation of MAPAs. Our results extend a recent study in yeast (Ruan *et al*, 2017) and suggest that the mitochondrial degradation of unfolded cytosolic proteins is a highly conserved mechanism. Through its interaction with FUNDC1, which serves as an anchor to the outer membrane of mitochondria, HSC70 can translocate many of its clients to the mitochondrial membrane or into the mitochondrial matrix, in addition to the known mitochondrial proteins. This translocation depends on the TOM/TIM complexes, and knockdown of either FUNDC1/HSC70 or TOM subunits will reduce protein translocation into mitochondria. Given the general role of HSC70 in recognizing unfolded proteins during normal proteostasis, it is conceivable that the FUNDC1/HSC70 axis may be active under normal conditions, and the translocated proteins would be degraded by LONP1 protease. Under proteostatic stress conditions, the mitochondrial translocation of unfolded cytosolic proteins is aggravated. Meanwhile, the interaction between FUNDC1 and HSC70 is enhanced due to dephosphorylation of FUNDC1 at Ser13, suggesting that the mitochondrial translocation of unfolded cytosolic proteins may be controlled by regulating the FUNDC1/HSC70 interaction through modifying the phosphorylation status of FUNDC1 at Ser13. Our findings thus propose the FUNDC1/HSC70 interaction as a novel connection between the cytosolic proteostasis network and mitochondrial quality control systems.

In this study, we employed R-GFP as a reporter for proteasomal degradation. Although R-GFP is an N-end rule substrate, HSC70 may also be involved in its proteasomal degradation, as knockdown of BAG1, a HSC70 co-chaperone that mediates the interaction between HSC70 and proteasome, caused accumulation of R-GFP (Gamerding *et al*, 2009). In line with this, we found that R-GFP can interact with HSC70 in a PBD-dependent manner, suggesting that R-GFP is also a HSC70 client. We also found that HSC70 can interact with UBR1 and knockdown of *UBR1* reduced the interaction between HSC70 and R-GFP (unpublished observation). These data

Figure 8. FUNDC1 is required for the autophagic degradation of MAPAs.

- A HeLa cells were transfected with GFP-LC3, treated with DMSO or 10 μ M MG132 for 8 h, and immunostained with anti-p62 antibody. Scale bar = 10 μ m.
- B Immunoblot analysis of the TCL of HeLa cells treated with MG132 as indicated.
- C Immunoblot analysis of the TCL of HeLa cells stably transfected with Ctrl or ATG5 shRNA and treated with MG132 as indicated.
- D Immunoblot analysis of the TCL of HeLa cells stably transfected with the indicated vectors and treated with MG132 as indicated.
- E Quantification of the results from panels (D and E). three replicates were analyzed using Student's two-tailed t-test and are presented as the means \pm SEM. * P < 0.05, ** P < 0.01, *** P < 0.001.
- F HeLa cells were stably transfected with the indicated vectors, transiently transfected with GFP-LC3 and then treated with 10 μ M MG132 for 8 h and immunostained with anti-p62 antibody. Scale bar = 10 μ m.
- G TEM analysis of F1 shRNA/F1-Myc or F1 shRNA/ Δ LIR-Myc cells treated with MG132 for 8 h. Yellow arrowheads show the MAPAs. Blue arrows show the places where membrane is absent. White arrowheads show the layered aggregates budding from mitochondria. Scale bar = 500 nm; M, mitochondrion.

Source data are available online for this figure.

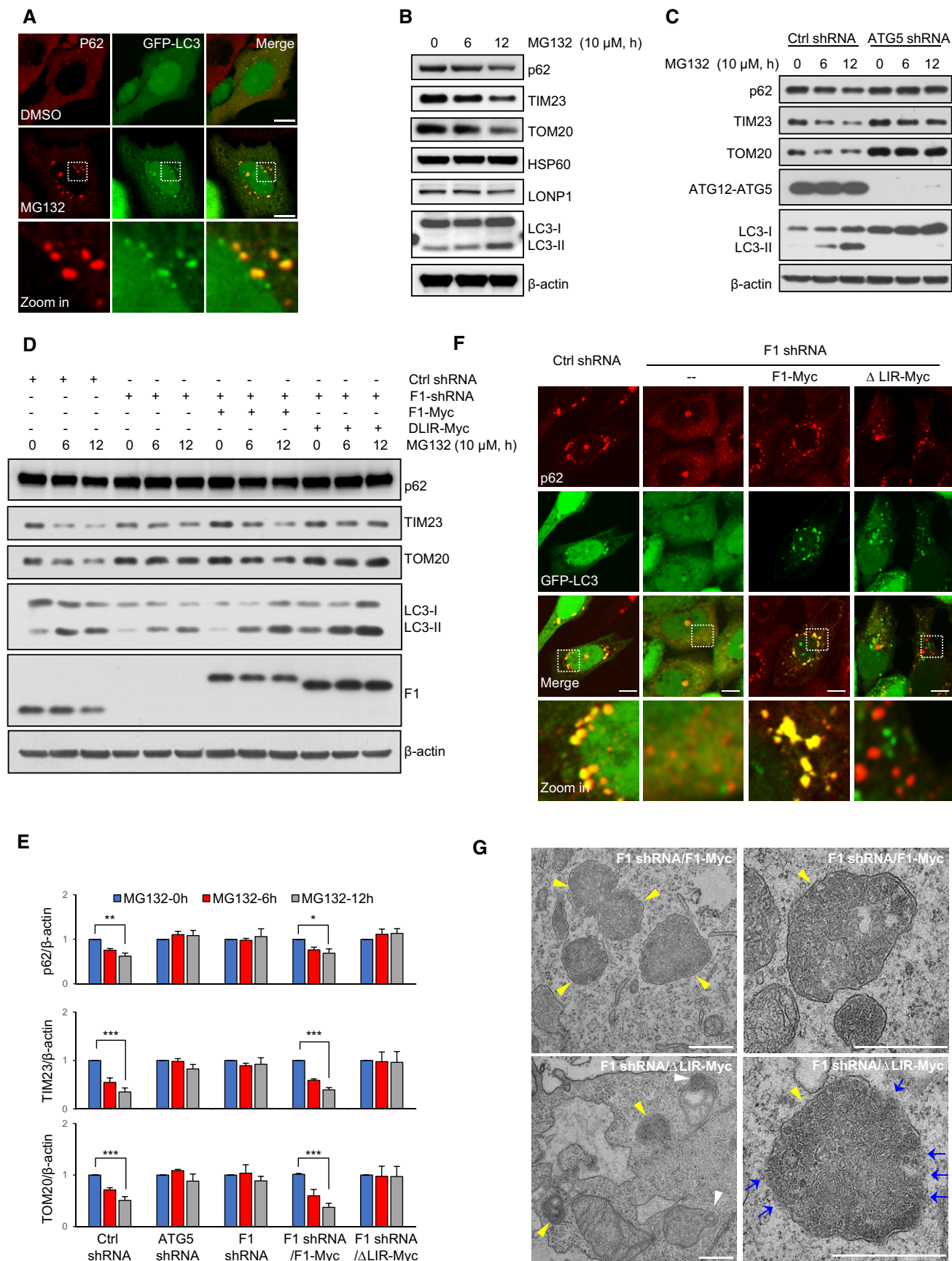


Figure 8.

are consistent with the phenotype in yeast that Ubr1 and Ubr2 can also promote the ubiquitination and degradation of the cytosolic unfolded or misfolded proteins with the assistance of HSP70 (Heck *et al*, 2010; Nillegoda *et al*, 2010). Hence, HSC70 may recognize R-GFP through the interaction with UBR1, although the precise mechanisms require further investigation.

It is well known that upon proteotoxic stress, protein aggregates are translocated to the centrosome region and colocalize with γ -tubulin (Johnston *et al*, 1998; Kopito, 2000). HSP70 is required for the formation of aggresomes (Zhang & Qian, 2011). Here, we describe the formation of a novel type of protein aggregates, which is dependent on FUNDC1/HSC70 pathway and is distinct from aggresome. MAPA formation was blocked by knockdown of FUNDC1, HSC70, or TOM complex components, while exacerbated by knockdown of LONP1 and HSP70. We thus suggest that mitochondria play a central role in organizing the formation of MAPAs, depending on the mitochondrial translocation of the unfolded cytosolic proteins. Interestingly, we showed that HSC70 and HSP70 cooperate in handling the misfolded proteins in a competitive fashion. Knockdown of HSC70 reduces MAPA formation, while knockdown of HSP70 promotes MAPA formation. The opposite effects of HSC70 and HSP70 on MAPA formation may attribute to their opposite effects on mitochondrial translocation of unfolded cytosolic proteins and different affinities for FUNDC1.

We found that MAPAs contain mitochondrial components, including some mitochondrial membrane proteins and unfolded proteins in the mitochondrial matrix, in addition to ubiquitinated proteins and p62. And it should also be noticed that FIS1 is required for the formation of MAPAs, suggesting a potential role of the mitochondrial fission machinery in MAPA formation. The expression of misfolding-prone OTC- Δ alone fails to induce MAPAs, suggesting that MAPA formation requires cooperation across the mitochondrial double membrane. We propose that the unfolded cytosolic proteins imported into mitochondria, if not

degraded by LONP1, may concentrate in certain regions and then become segregated from the mitochondria in a FIS1-dependent manner to form MAPAs in combination with the ubiquitinated proteins and p62 at the outer membrane of mitochondria. The mitochondrial membrane proteins, especially FUNDC1, may be incorporated into the MAPAs during this process. The exact molecular nature of MAPAs and the mechanism of their formation warrant further investigation.

p62 is known as an autophagy receptor that recognizes cargos by binding to ubiquitin via its UBA domain and tethers these cargos to the autophagic degradation machinery by directly binding to LC3 (Pankiv *et al*, 2007). It is commonly detected in ubiquitinated protein aggregates in cultured cells and Lewy bodies and other intraneuronal inclusions in neuronal diseases (Kuusisto *et al*, 2001; Zatloukal *et al*, 2002; Nagaoka *et al*, 2004; Nakano *et al*, 2004). In this study, we showed that deletion of the FUNDC1 LIR had no effect on the formation of p62-positive MAPAs, while abolished the colocalization between p62 and LC3 and degradation of MAPA-localized proteins such as p62, TIM23, and TOM20, suggesting that FUNDC1 is required for the recognition of MAPAs by autophagosomes. Our results are in line with recent studies, suggesting that both p62 and NBR1 are dispensable for the clearance of aggresomes and other protein aggregates (Wong *et al*, 2012). We thus reveal a new function for FUNDC1 in aggrephagy under proteostatic stress conditions, in addition to its intrinsic role in mitophagy under hypoxic conditions.

Impairment of the proteostatic network and mitochondrial dysfunction are two drivers for aging and age-associated diseases, but the interconnections between these two systems are not well characterized. A number of studies have shown that proteasome inhibition is capable of inducing mitochondrial dysfunction, ROS generation, and senescence-like phenotypes in individual cells (Ling *et al*, 2003; Chondrogianni & Gonos, 2004; Pei *et al*, 2004; Sullivan *et al*, 2004; Chondrogianni *et al*, 2008; Torres & Perez, 2008). In line with this, genetic or pharmaceutical activation of the

Figure 9. Roles of FUNDC1, HSC70, HSP70, Bcl-xL, LONP1, and FIS1 in MG132-induced cell senescence.

- A, B HeLa cells were treated with DMSO or 10 μ M MG132 for 8 h and then washed with fresh medium three times and cultured for another 3 days. Cells were then fixed and subjected to SA- β -gal staining. The senescent cells show SA- β -gal-positive staining (Blue). Quantification is shown in (B).
- C, D Immunoblot analysis of HeLa cells treated with DMSO or MG132 for 8 h and then washed and cultured for the indicated times. Quantification is shown in (D).
- E, F Quantification of SA- β -gal staining in HeLa cells treated with DMSO or MG132 for 8 h and then washed and incubated in fresh medium containing DMSO or Compound C (C.C) for another 3 days. Immunoblot analysis of the cells is shown in (F).
- G, H Quantification of SA- β -gal staining of HeLa cells stably transfected with the indicated vectors, treated with DMSO or MG132 for 8 h and then washed and cultured for 3 days. Immunoblot analysis of the cells is shown in (H). The up-regulation of p53 and p21 at 3 days after pulse treatment with MG132 was alleviated by FUNDC1 knockdown and restored by reintroduction of F1-Myc or Δ LIR-Myc, although the basal level of p53 in FUNDC1-knockdown cells is higher than that in control cells.
- I, J Quantification of MG132-induced SA- β -gal staining in HeLa cells stably transfected with Ctrl, HSP70, or HSC70 shRNA, treated with DMSO or MG132 for 8 h and then washed and cultured for 3 days. Immunoblot analysis of the cells is shown in (J). The up-regulation of p53 and p21 at 3 days after pulse treatment with MG132 was alleviated by HSC70 knockdown, although the basal level of p53 in HSC70-knockdown cells is higher than that in control cells. Both p53 and p21 were up-regulated in HSP70-knockdown cells treated with or without MG132.
- K, L HeLa cells stably transfected with tetracycline (Tet)-inducible Bcl-xL expression vector were incubated in DMEM containing Tet or not for 12 h, then treated with DMSO or 10 μ M MG132 for 8 h, and then washed and incubated in fresh medium for another 3 days. Cells were then subjected to SA- β -gal staining. Immunoblot analysis of the cells is shown in (L). The induced Bcl-xL was detectable even 3 days after treatment withdrawal, because this protein is stable.
- M, N Quantification of the SA- β -gal staining of HeLa cells stably transfected with Ctrl or LONP1 shRNA, treated with DMSO or MG132 for 8 h and then washed and cultured for 3 days. Immunoblot analysis of the cells is shown in (N).
- O, P Quantification of the SA- β -gal staining of HeLa cells stably transfected with Ctrl or FIS1 shRNA, treated with DMSO or MG132 for 8 h and then washed and cultured for 3 days. Immunoblot analysis of the cells is shown in (P).

Data information: In panels (B, D, E, G, I, K, M and O), three replicates were analyzed using Student's two-tailed *t*-test and are presented as the means \pm SEM. **P* < 0.05; ***P* < 0.01; ****P* < 0.001.

Source data are available online for this figure.

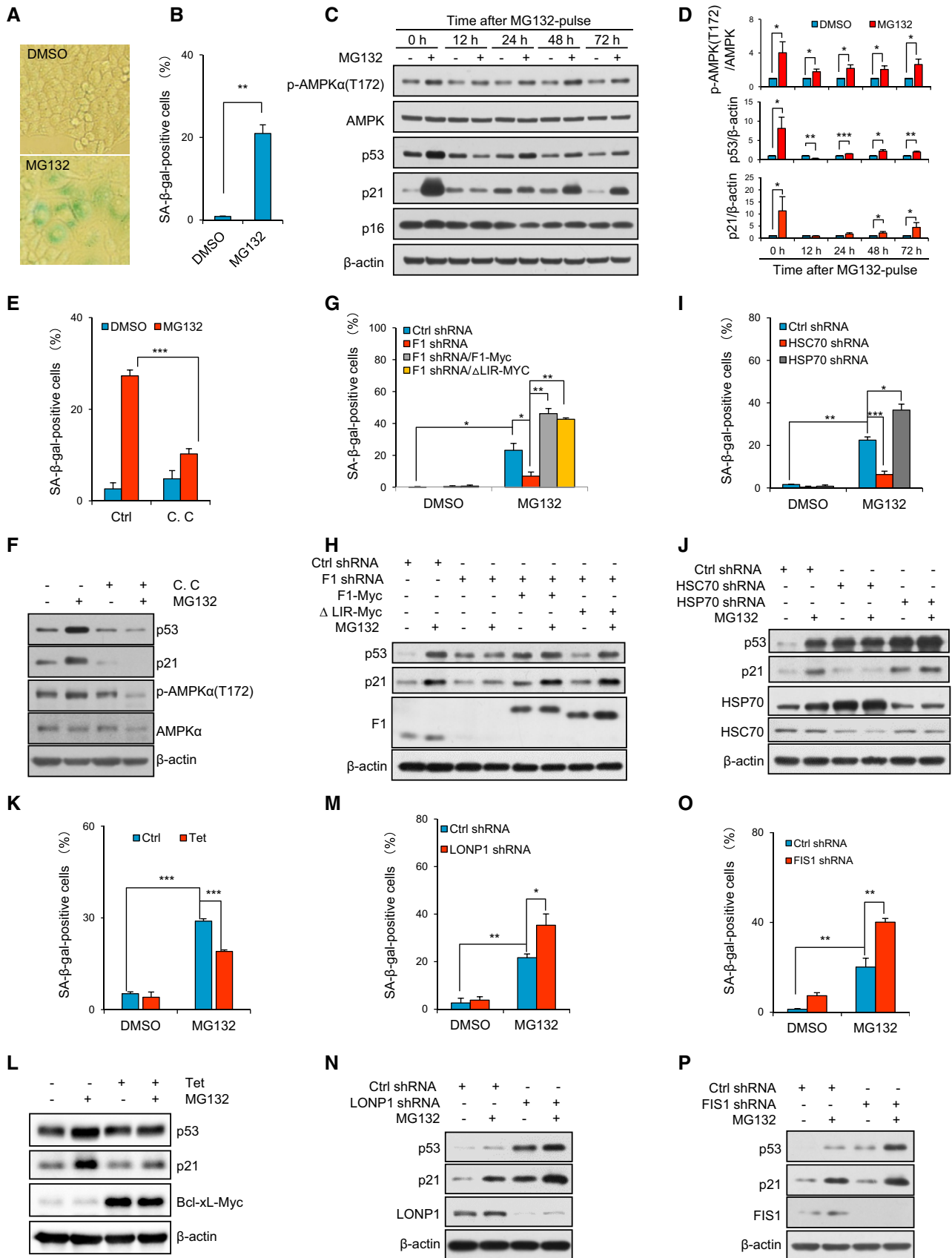


Figure 9.

proteasome retards cell senescence, the cellular basis for aging (Chondrogianni *et al*, 2014). Previous work has tried to explain these phenomena by investigating the role of the proteasome in degrading mitochondrial proteins, especially the outer mitochondrial membrane (OMM) proteins and mistargeted mitochondrial protein precursors. In this study, we found that mitochondria can be directly targeted by misfolded proteins, rendering cells susceptible to proteotoxicity and senescence. Knockdown of FUNDC1 and HSC70 impeded the translocation of client proteins to mitochondria and alleviated the senescence-like phenotypes. In contrast, knockdown of HSP70, LONP1, and FIS1 increased the accumulation of client proteins in mitochondria and exacerbated the senescence-like phenotypes. In particular, knockdown of FIS1 enhances misfolded protein accumulation without much MAPA formation, suggesting that the accumulation of misfolded proteins in the mitochondrial matrix, rather than the MAPA formation, is probably responsible for the occurrence of cell senescence. Our results thus provide a missing link that can explain how impaired proteostasis causes mitochondrial dysfunction and consequent cell senescence and aging.

Materials and Methods

Cell culture and transfection

HeLa, U2OS, and HepG2 cells were grown in DMEM (Hyclone) containing 10% fetal bovine serum and antibiotics at 37°C under 5% CO₂. Plasmid transfection was performed using MegaTran 1.0 (OriGene, TT200003) following the manufacturer's instructions. Primers for shRNA were designed following the manufacturer's instructions and cloned into the pSilencer2.1-neo vector to construct the shRNA against HSC70, HSP70, LONP1, FIS1, and CLPP. Primers for shRNA were designed following the manufacturer's instructions and cloned into the pSUPER.retro.puro and pSUPER-nGFP.vector to construct the shRNA against TOM20, TOM22, and TOM70. The target sequence in HSC70 is 5'-CTGACAAAGATGAAGGAAA-3', in CHIP is 5'-AGGCCAAGCAGACAAGTA-3', and in LONP1 is 5'-GGACCTCAGTCGGCTTAAT-3'. The shRNA target sequences in FUNDC1, HSP70, FIS1, CLPP, Drp1, TOM20, TOM22, and TOM70 are as described (Gandre-Babbe & van der Bliek, 2008; Cheng *et al*, 2009; Kita *et al*, 2012; Liu *et al*, 2012a; Zhuang *et al*, 2013; Chen *et al*, 2016). To establish stable knockdown cell lines, HeLa cells were transfected with the corresponding shRNA vectors and selected with neomycin. FUNDC1-knockdown cells were transfected with FUNDC1-Myc and FUNDC1-ΔLIR-Myc expression plasmids and selected with zeocin to establish stable rescued cell lines. FUNDC1-knockout cells were established using CRISPR/Cas9 system and verified through immunoblotting analysis.

Reagents and antibodies

See Appendix Supplementary Methods.

Fraction analysis and Proteinase K protection assay

HeLa cells treated with DMSO or 10 μM of MG132 for 4 h or transfect with certain vectors were harvested and washed with PBS, resuspended in 1 ml of isolation buffer (IB) (10 mM Tris-MOPS, 1 mM

EGTA-Tris, 200 mM sucrose, 1 mM PMSF, pH 7.4), lysed by passing through a 29 G needle attached to 1-ml syringe 12 times, and centrifuged for 10 min at 800 g, 4°C. The supernatant was transferred to fresh tubes and centrifuged for 10 min at 10,000 g, 4°C. The pellets were then resuspended in 50 μl of IB and dissolved in SDS sample buffer and boiled to make the mitochondrial fraction samples. 6 × SDS sample buffer was added to the supernatants, which were boiled to make the cytosol samples. Samples were then analyzed by SDS-PAGE and Western blotting. To make the total cell lysates (TCL), cells were directly boiled in SDS sample buffer and then subjected to Western blotting analysis to detect the levels of proteins in whole cells.

To trace the sub-mitochondrial locations of the related proteins, mitochondria were treated with 100 μg/ml of proteinase K (Pro. K) in the presence of 0.1% digitonin or 1% Triton X-100 (or not) in 30 μl of IB for 15 min at room temperature. 7 mM PMSF was added for 5 min to inactivate Protease K. 5 μl of 6 × SDS sample buffer was added, and the samples were boiled and analyzed by SDS-PAGE and Western blotting.

In vitro import assay

Cytosolic fractions isolated from GFP- or Ub-R-GFP-expressing cells were mixed with mitochondria isolated from the untreated HeLa cells and then incubated at room temperature for 1 h, and mitochondria were isolated via centrifugation and subjected to immunoblot analysis. To check the suborganellar localization of R-GFP, mitochondria isolated from the *in vitro* system were treated with 100 μg/ml of Pro. K for 15 min at room temperature before immunoblot analysis.

Differential detergent fractionation

HeLa cells treated with DMSO or MG132 were harvested and lysed in Triton X-100 lysis buffer (50 mM NaCl, 10 mM Tris pH 7.5, 5 mM EDTA, and 1% Triton X-100) and then centrifuged at 17,000 × g for 15 min at 4°C. The supernatants (TX-soluble fraction) and the pellets (TX-insoluble fraction) were collected and analyzed by immunoblotting.

Ni²⁺-NTA precipitation assay

For immunoprecipitation, Ni²⁺-NTA precipitation, and protein oxidation detection, cells were dissolved in lysis buffer containing 50 mM Tris-HCl (pH 7.4), 137 mM NaCl, 2 mM EDTA, 10% glycerol, 1 mM PMSF, and 1% NP-40. The lysates were centrifuged at 10,000 × g for 15 min, and the supernatants were collected for further use.

Cell lysates were incubated with Ni²⁺-NTA beads with rotation for 2 h at 4°C. The beads were pelleted by spinning, washed with lysis buffer three times and subjected to SDS-PAGE separation and Coomassie Brilliant Blue staining.

Immunoprecipitation

Cells were lysed as described above, and then, primary antibodies were added to the lysates and incubated with rotation for 2 h at 4°C. A 50% slurry of protein G-Sepharose was then added, and the incubation was continued for an additional 4 h. After washing three times with ice-cold lysis buffer, the precipitates were subjected to Western blotting analysis.

SA- β -gal staining

Cells treated with DMSO or 10 μ M of MG132 for 8 h were washed with fresh medium three times and cultured for 3 days. SA- β -gal staining was performed using the Senescence β -Galactosidase Staining Kit (Beyotime, C0602) following the manufacturer's instructions. SA- β -gal-positive cells were evaluated by watching under microscope. For each sample, > 100 cells from five random visual fields were analyzed, percentage of the β -gal-positive cells were calculated, and means \pm SEM of three independent experiments are shown.

Protein oxidation detection

Cells were lysed using the above-mentioned lysis buffer containing 50 mM DTT. The total protein concentration in the lysates was then quantitated and equalized. Five microliters of the lysates was subjected to detection of oxidized proteins using the OxyBlot Protein Oxidation Detection Kit (Millipore, S7150) following the manufacturer's instructions.

SDS-PAGE and Western blotting

Samples were subjected to SDS-PAGE and transferred to nitrocellulose membranes. The membranes were then blocked and incubated with appropriate primary antibodies followed by HRP-conjugated secondary antibodies. Immunoblotted bands were visualized with a chemiluminescence kit (Thermo Fisher, 32109).

Immunofluorescence staining

Cells were seeded onto coverslips and fixed with 4% paraformaldehyde in PBS and then permeabilized with 0.2% Triton X-100. After incubation with 2% BSA in PBS, the cells were incubated with the primary antibody (1:100) for 2 h and Alexa488-, Alexa555-, or Alexa647-conjugated secondary antibody (1:1,000) for 1 h. After washing with PBS, the cells were mounted and subjected to observation. For digitonin permeabilization, cells were incubated in 25 μ g/ml digitonin for 10 min on ice to remove cytosolic proteins before fixing.

Confocal microscopy

Both immunostained and live cells were observed with a confocal laser scanning microscope (Zeiss LSM510). Live cells were imaged in a temperature-controlled chamber (37°C) at 5% CO₂.

Transmission electron microscopy

See Appendix Supplementary Methods.

Cryogenic super-resolution correlative light and electron microscopy (csCLEM)

See Appendix Supplementary Methods.

Quantifications

Intensity of immunoblotting band was quantified by using ImageJ (National Institutes of Health), the ratios between the target proteins

and loading control were calculated and normalized, and means \pm SEM of three independent experiments are shown. The number of MAPAs in each cell was counted manually, and 30–50 cells from three independent experiments were analyzed for each group.

Statistical analysis

Data were analyzed using Student's two-tailed *t*-test and are presented as the means \pm SEM. Statistical significance was set at *P* < 0.05.

Expanded View for this article is available online.

Acknowledgements

We thank Dr. Xi Chen from the Microscale Reconstruction and Analysis group, Institute of Automation, Chinese Academy of Sciences, for developing the scanning map software for csCLEM. We thank Dr. Lusheng Gu and Weixing Li from the Center for Biological Instrument Development (CBID), Dr. Zhenxi Guo from Center for Biology Imaging, Core Facility for Protein Research, Institute of Biophysics, Chinese Academy of Sciences, for supporting the csCLEM system. We thank Yinzi Ma and Pengyan Xia for supporting the TEM assay. We wish to thank Y. Z. Luo from Tsinghua University for providing the HA-HSC70 construct. We thank B. Lv from Wenzhou Medical University for providing the LONP1 expression vector. The research was funded by the National Natural Science Foundation of China (31790404), Fund for Strategic Pilot Technology Chinese Academy of Sciences (XDPB1002), the Chinese Academy of Sciences Key project of Frontier Science (QYZDJSSW-SMC004) and the Ministry of Science and Technology of China (2016YFA0500201) to QC; National Key R & D Program of China (2017YFA0504700) to Yanhong Xue; National Natural Science Foundation of China (31471306) to LL; General Financial Grant from the China Postdoctoral Science Foundation (2013M541040) to Yanjun Li.

Author contributions

YLi performed most of the experiments and data analysis; YX, XX, WJ and TX performed the csCLEM; HW performed the co-IP analysis; WL, YW, LL, and ZC constructed the plasmids; GW, YLiu, YZ and WZ helped to perform the TEM experiment; and QC and YLi designed the experiments and wrote the manuscript.

Conflict of interest

The authors declare that they have no conflict of interest.

References

- Chen G, Han Z, Feng D, Chen Y, Chen L, Wu H, Huang L, Zhou C, Cai X, Fu C, Duan L, Wang X, Liu L, Liu X, Shen Y, Zhu Y, Chen Q (2014) A regulatory signaling loop comprising the PGAM5 phosphatase and CK2 controls receptor-mediated mitophagy. *Mol Cell* 54: 362–377
- Chen M, Chen Z, Wang Y, Tan Z, Zhu C, Li Y, Han Z, Chen L, Gao R, Liu L, Chen Q (2016) Mitophagy receptor FUNDC1 regulates mitochondrial dynamics and mitophagy. *Autophagy* 12: 689–702
- Cheng TL, Liao CC, Tsai WH, Lin CC, Yeh CW, Teng CF, Chang WT (2009) Identification and characterization of the mitochondrial targeting sequence and mechanism in human citrate synthase. *J Cell Biochem* 107: 1002–1015

- Chondrogianni N, Gonos ES (2004) Proteasome inhibition induces a senescence-like phenotype in primary human fibroblasts cultures. *Biogerontology* 5: 55–61
- Chondrogianni N, Trougakos IP, Kletsas D, Chen QM, Gonos ES (2008) Partial proteasome inhibition in human fibroblasts triggers accelerated M1 senescence or M2 crisis depending on p53 and Rb status. *Aging Cell* 7: 717–732
- Chondrogianni N, Sakellari M, Lefaki M, Papaevgeniou N, Gonos ES (2014) Proteasome activation delays aging *in vitro* and *in vivo*. *Free Radic Biol Med* 71: 303–320
- Ciani B, Layfield R, Cavey JR, Sheppard PW, Searle MS (2003) Structure of the ubiquitin-associated domain of p62 (SQSTM1) and implications for mutations that cause Paget's disease of bone. *J Biol Chem* 278: 37409–37412
- Connell P, Ballinger CA, Jiang J, Wu Y, Thompson LJ, Hohfeld J, Patterson C (2001) The co-chaperone CHIP regulates protein triage decisions mediated by heat-shock proteins. *Nat Cell Biol* 3: 93–96
- Dantuma NP, Lindsten K, Glas R, Jellne M, Masucci MG (2000) Short-lived green fluorescent proteins for quantifying ubiquitin/proteasome-dependent proteolysis in living cells. *Nat Biotechnol* 18: 538–543
- Fischer F, Hamann A, Osiewacz HD (2012) Mitochondrial quality control: an integrated network of pathways. *Trends Biochem Sci* 37: 284–292
- Fourie AM, Sambrook JF, Gething MJ (1994) Common and divergent peptide binding specificities of hsp70 molecular chaperones. *J Biol Chem* 269: 30470–30478
- Gamerding M, Hajieva P, Kaya AM, Wolfrum U, Hartl FU, Behl C (2009) Protein quality control during aging involves recruitment of the macroautophagy pathway by BAG3. *EMBO J* 28: 889–901
- Gandre-Babbe S, van der Blik AM (2008) The novel tail-anchored membrane protein Mff controls mitochondrial and peroxisomal fission in mammalian cells. *Mol Biol Cell* 19: 2402–2412
- Ganguly G, Chakrabarti S, Chatterjee U, Saso L (2017) Proteinopathy, oxidative stress and mitochondrial dysfunction: cross talk in Alzheimer's disease and Parkinson's disease. *Drug Des Devel Ther* 11: 797–810
- Hartl FU, Bracher A, Hayer-Hartl M (2011) Molecular chaperones in protein folding and proteostasis. *Nature* 475: 324–332
- Heck JW, Cheung SK, Hampton RY (2010) Cytoplasmic protein quality control degradation mediated by parallel actions of the E3 ubiquitin ligases Ubr1 and San1. *Proc Natl Acad Sci USA* 107: 1106–1111
- Hytinen JM, Amadio M, Viiri J, Pascale A, Salminen A, Kaarniranta K (2014) Clearance of misfolded and aggregated proteins by aggrephagy and implications for aggregation diseases. *Ageing Res Rev* 18: 16–28
- Johnston JA, Ward CL, Kopito RR (1998) Aggresomes: a cellular response to misfolded proteins. *J Cell Biol* 143: 1883–1898
- Kaushik S, Cuervo AM (2015) Proteostasis and aging. *Nat Med* 21: 1406–1415
- Khaminets A, Behl C, Dikic I (2016) Ubiquitin-dependent and independent signals in selective autophagy. *Trends Cell Biol* 26: 6–16
- Kita K, Suzuki T, Ochi T (2012) Diphenylarsinic acid promotes degradation of glutaminase C by mitochondrial Lon protease. *J Biol Chem* 287: 18163–18172
- Koga H, Kaushik S, Cuervo AM (2011) Protein homeostasis and aging: the importance of exquisite quality control. *Ageing Res Rev* 10: 205–215
- Kopito RR (2000) Aggresomes, inclusion bodies and protein aggregation. *Trends Cell Biol* 10: 524–530
- Kuusisto E, Salminen A, Alafuzoff I (2001) Ubiquitin-binding protein p62 is present in neuronal and glial inclusions in human tauopathies and synucleinopathies. *NeuroReport* 12: 2085–2090
- Lim J, Yue Z (2015) Neuronal aggregates: formation, clearance, and spreading. *Dev Cell* 32: 491–501
- Ling YH, Liebes L, Zou Y, Perez-Soler R (2003) Reactive oxygen species generation and mitochondrial dysfunction in the apoptotic response to Bortezomib, a novel proteasome inhibitor, in human H460 non-small cell lung cancer cells. *J Biol Chem* 278: 33714–33723
- Liu L, Feng D, Chen G, Chen M, Zheng Q, Song P, Ma Q, Zhu C, Wang R, Qi W, Huang L, Xue P, Li B, Wang X, Jin H, Wang J, Yang F, Liu P, Zhu Y, Sui S et al (2012a) Mitochondrial outer-membrane protein FUNDC1 mediates hypoxia-induced mitophagy in mammalian cells. *Nat Cell Biol* 14: 177–185
- Liu T, Daniels CK, Cao S (2012b) Comprehensive review on the HSC70 functions, interactions with related molecules and involvement in clinical diseases and therapeutic potential. *Pharmacol Ther* 136: 354–374
- Liu B, Xue Y, Zhao W, Chen Y, Fan C, Gu L, Zhang Y, Zhang X, Sun L, Huang X, Ding W, Sun F, Ji W, Xu T (2015) Three-dimensional super-resolution protein localization correlated with vitrified cellular context. *Sci Rep* 5: 13017
- Lystad AH, Simonsen A (2015) Assays to monitor aggrephagy. *Methods* 75: 112–119
- Mizushima N, Levine B, Cuervo AM, Klionsky DJ (2008) Autophagy fights disease through cellular self-digestion. *Nature* 451: 1069–1075
- Mizushima N, Yoshimori T, Levine B (2010) Methods in mammalian autophagy research. *Cell* 140: 313–326
- Nagaoka U, Kim K, Jana NR, Doi H, Maruyama M, Mitsui K, Oyama F, Nukina N (2004) Increased expression of p62 in expanded polyglutamine-expressing cells and its association with polyglutamine inclusions. *J Neurochem* 91: 57–68
- Nakano T, Nakaso K, Nakashima K, Ohama E (2004) Expression of ubiquitin-binding protein p62 in ubiquitin-immunoreactive intraneuronal inclusions in amyotrophic lateral sclerosis with dementia: analysis of five autopsy cases with broad clinicopathological spectrum. *Acta Neuropathol* 107: 359–364
- Nillegoda NB, Theodoraki MA, Mandal AK, Mayo KJ, Ren HY, Sultana R, Wu K, Johnson J, Cyr DM, Caplan AJ (2010) Ubr1 and Ubr2 function in a quality control pathway for degradation of unfolded cytosolic proteins. *Mol Biol Cell* 21: 2102–2116
- Pandey UB, Nie Z, Batlevi Y, McCray BA, Ritson GP, Nedelsky NB, Schwartz SL, DiProspero NA, Knight MA, Schuldiner O, Padmanabhan R, Hild M, Berry DL, Garza D, Hubbert CC, Yao TP, Baehrecke EH, Taylor JP (2007) HDAC6 rescues neurodegeneration and provides an essential link between autophagy and the UPS. *Nature* 447: 859–863
- Pankiv S, Clausen TH, Lamark T, Brech A, Bruun JA, Outzen H, Overvatn A, Bjorkoy G, Johansen T (2007) p62/SQSTM1 binds directly to Atg8/LC3 to facilitate degradation of ubiquitinated protein aggregates by autophagy. *J Biol Chem* 282: 24131–24145
- Pei XY, Dai Y, Grant S (2004) Synergistic induction of oxidative injury and apoptosis in human multiple myeloma cells by the proteasome inhibitor bortezomib and histone deacetylase inhibitors. *Clin Cancer Res* 10: 3839–3852
- Ross JM, Olson L, Coppotelli G (2015) Mitochondrial and ubiquitin proteasome system dysfunction in ageing and disease: two sides of the same coin? *Int J Mol Sci* 16: 19458–19476
- Ruan L, Zhou C, Jin E, Kucharavy A, Zhang Y, Wen Z, Florens L, Li R (2017) Cytosolic proteostasis through importing of misfolded proteins into mitochondria. *Nature* 543: 443–446
- Ryan MT, Hoogenraad NJ (2007) Mitochondrial-nuclear communications. *Annu Rev Biochem* 76: 701–722

- Sullivan PG, Dragicevic NB, Deng JH, Bai Y, Dimayuga E, Ding Q, Chen Q, Bruce-Keller AJ, Keller JN (2004) Proteasome inhibition alters neural mitochondrial homeostasis and mitochondria turnover. *J Biol Chem* 279: 20699–20707
- Torres CA, Perez VI (2008) Proteasome modulates mitochondrial function during cellular senescence. *Free Radic Biol Med* 44: 403–414
- Voos W (2009) Mitochondrial protein homeostasis: the cooperative roles of chaperones and proteases. *Res Microbiol* 160: 718–725
- Wong E, Bejarano E, Rakshit M, Lee K, Hanson HH, Zaarur N, Phillips GR, Sherman MY, Cuervo AM (2012) Molecular determinants of selective clearance of protein inclusions by autophagy. *Nat Commun* 3: 1240
- Wu H, Xue D, Chen G, Han Z, Huang L, Zhu C, Wang X, Jin H, Wang J, Zhu Y, Liu L, Chen Q (2014) The BCL2L1 and PGAM5 axis defines hypoxia-induced receptor-mediated mitophagy. *Autophagy* 10: 1712–1725
- Youle RJ, Narendra DP (2011) Mechanisms of mitophagy. *Nat Rev Mol Cell Biol* 12: 9–14
- Zatloukal K, Stumptner C, Fuchsichler A, Heid H, Schnoelzer M, Kenner L, Kleinert R, Prinz M, Aguzzi A, Denk H (2002) p62 Is a common component of cytoplasmic inclusions in protein aggregation diseases. *Am J Pathol* 160: 255–263
- Zhang X, Qian SB (2011) Chaperone-mediated hierarchical control in targeting misfolded proteins to aggresomes. *Mol Biol Cell* 22: 3277–3288
- Zhao Q, Wang J, Levichkin IV, Stasinopoulos S, Ryan MT, Hoogenraad NJ (2002) A mitochondrial specific stress response in mammalian cells. *EMBO J* 21: 4411–4419
- Zhuang H, Jiang W, Zhang X, Qiu F, Gan Z, Cheng W, Zhang J, Guan S, Tang B, Huang Q, Wu X, Huang X, Jiang W, Hu Q, Lu M, Hua ZC (2013) Suppression of HSP70 expression sensitizes NSCLC cell lines to TRAIL-induced apoptosis by upregulating DR4 and DR5 and downregulating c-FLIP-L expressions. *J Mol Med (Berl)* 91: 219–235